



MAX-PLANCK-GESELLSCHAFT



Part A

2.1.10 Carbons

Prof. Dr. R. Schlögl

Department of Inorganic Chemistry, Fritz-Haber-Institute of the MPG, Faradayweg 4-6, 14195 Berlin, Germany

Corresponding author: e-mail schloegl@fhi-berlin.mpg.de, phone +49 30 8413 4400, fax +49 30 8413 4401

2.1.10.1. Introduction

The element carbon plays a multiple role in heterogeneous catalysis. In homogeneous catalysis it occurs of course as the most prominent constituent of ligand systems and will be treated as such there. Carbon-containing molecules are, in most catalytic applications, the substrates of the process under consideration. Deposits and polymers of carbon often occur as poisons on catalysts. Carbon deposition is the most severe problem in certain zeolite applications. In hydrogenation reactions carbon deposits are thought to act as modifiers for the activity of the catalyst and to provide selectivity by controlling the hydrogenation-dehydrogenation activity of the metal part of the catalyst. Carbon deposits are even thought to constitute part of the active sites in some cases.

Carbon is a prominent catalyst support material as it allows the anchoring of metal particles on a substrate which does not exhibit solid acid-base properties. Carbon is finally a catalyst in its own right allowing the activation of oxygen and chlorine for selective oxidation, chlorination and de-chlorination reactions.

These multiple roles of the element carbon are in parallel with a complex structural chemistry giving rise to families of chemically vastly different modifications of the element. It is a special characteristic of carbon chemistry that many of these modifications cannot be obtained as phase-pure materials. This limits the exact knowledge of physical and chemical properties to a few archetype modifications, namely graphite and diamond.

The reason for this poor definition of materials is found in the process of its formation. This is comprised of

difficult to control polymerisation reactions. Such reactions will occur also in catalytic reactions with small organic molecules. The nature of carbon deposits will therefore reflect all the complexity of the bulk carbon materials. It is one aim of this article to describe the structural and chemical complexity of "carbon" or "soot" in order to provide an understanding of the frequently observed complexity of the chemical reactivity (e.g. in re-activation processes aiming at an oxidative removal of deposits).

The surface chemistry of carbon which determines its interfacial properties is a rich field as a wide variety of surface functional groups are known to exist on carbon. The by far most important family of surface functional groups are those involving oxygen. Other prominent heteroatoms on the surface are hydrogen and nitrogen. This article focusses on the description and characterisation of oxygen surface functional groups.

In the final section, selected case studies of carbon chemistry in catalysis will be discussed in order to illustrate characteristic properties of carbon materials as wanted or unwanted components in catalytic systems.

Regarding the literature on basic properties of carbon materials, the reader is referred to the extensive collection of review papers published in the series

Chemistry and Physics of Carbon. Editors P.L. Walker and P.A. Thrower, Marcel Dekker, New York (presently 26 volumes, is continuing).

Fundamental on structural, physical and chemical properties of carbon allotropes are the following books:

"Physics of Graphite" B.T. Kelly, *Applied Science, London (1981)*

“Properties of Diamond”, J.E. Field, Academic Press, London, (1979)

*“Science of Fullerenes and Carbon Nanotubes”
M.S. Dresselhaus, G. Dresselhaus, P.C. Eklund,
Academic Press (1996)*

Many relevant investigations on material properties of carbons can be found in the specialised Journal “Carbon” which occurs in 1996 in its 34th volume. Relevant for chemical and catalytic issues is further the Journal “Fuel”, which occurs in 1996 in its 75th issue.

2.1.10.2. Structural Chemistry of Carbon Modifications

The chemistry of the element carbon is extremely complex both in the molecules and in the solid state. The reason for this complexity lies in the pronounced tendency of the element to form homonuclear bonds in three various bonding geometries. They can either occur uniformly or in almost unlimited combinations allowing a very large number of homonuclear structures of elemental carbon called “modifications”. The moderate electronegativity of carbon allows for strong covalent interactions with all main group elements. This adds enormously to the complexity of the solid-state chemistry of carbon. In the present context the carbon-oxygen bonds will be treated in more detail as these bond determine to a large extent the stability and reactivity of carbon in typical “catalytic” environments.

A consequence of the wide choice of bonding situations for carbon atoms is that only very few modifications can be prepared with any degree of purity complicating the determination of structural, chemical and physical properties. This is illustrated by the fact that even the crystal structure of graphite is only an approximate model [1] as no single crystal with low enough defect concentrations was ever found to allow a regular three-dimensional X-ray structure determination. In the context of catalysis it is important to note that “black carbon”, “coke”, “soot” or “carbonaceous deposit” is by no means a graphitic or even homogeneous material with reproducible properties. This leads into alia to the wide variations in application profiles of synthetic carbon blacks (several thousand varieties) and to the difficulties in the determination of oxidation properties of “coke” on catalyst surfaces.

2.1.10.3. An Overview

The carbon atom with its electron configuration $2s^2, 2p^2$ can form a maximum of 4 bonds which can be either single, double or triple bonds. As a result three main connectivities depicted in Figure 1 result. The valence orbitals hybridise, forming in the elemental state, sp , sp^2 or sp^3 hybrid orbitals. The data in Figure 1 illustrate that the local bonding geometry and the carbon-carbon bond distances vary significantly with the connectivity as the bond order (and

bond strength) increases from the sp^3 to the sp hybridisation state.

The tetrahedral connectivity leads to space-filling carbon polymers which are realised as defect-free ideal structures in diamond. The trigonal connectivity leads to sheets of carbon which are, in the defect-free variety, made up of hexagons leading to so-called graphene layers. The structures of graphite will result if these layers are regularly stacked in the third dimension. In the trigonal connectivity the sp^2 hybrid orbitals leave one non-bonding atomic orbital per carbon atom. These orbitals can interact with each other forming so-called “weak bonds”. These weak bonds can either interact as isolated or conjugated localised double bonds as in alkene molecules or as delocalised “aromatic” bonds providing metallic properties as in graphite. Any combination between these ideal interactions in defective carbons occurs within areas of double bond character and areas of aromatic character within one carbon sheet. In molecular chemistry this effect of varying degree of double bond localisation is referred to as “mesomerism”. This is rarely observed experimentally (in certain polycyclic aromatic molecules) due to the limited size of organic molecules. A further consequence of the existence of the weak bonds is the action of strong dispersive forces or “van der Waals” bonds in successive layers allowing for the cohesion of graphene layers. These forces provide energy for chemisorption of both polar and non-polar molecules on graphite surfaces. The bonding strength of the planar connectivity leads to a very poor chemical reactivity of graphene layers which can, at chemical energies, only be reactive at their edges where the lack of carbon atoms results into dangling bonds.

The trigonal connectivity leads not only to hexagons but enables the incorporation of triangles, pentagons, heptagons and larger cyclic structures as local defects into the honeycomb basic structure. A consequence of these defects is the strong localisation of double bonds around these defects and the deviation of the carbon sheet from planarity. Three-dimensional bends require the incorporation of non-hexagonal units in carbon layers. These form preferred centres of chemical reactivity as the localised double bonds will behave like alkene molecules in organic chemistry showing pronounced reactivity towards addition and insertion as compared to the typical substitution chemistry of aromatic structures.

The linear connectivity of sp hybridisation leads to chain-like polymers with conjugated triple bonds formed by the two sets of orthogonal non-bonding orbitals as shown in Figure 1. The resulting structure of cumulated electron density creates high chemical reactivity towards restructuring into the trigonal or tetragonal connectivity and towards addition of heteroatoms. A re-distribution of the weak-bonding electrons as found in molecular ketenes does not occur in pure carbon materials. The inherent chemical instability of this arrangement causes the materials to occur, under ambient conditions, only rarely in pure form after rapid quenching from high-temperature carbon sources or in meteorites. These phases (e.g. “chaotit”) are

thermodynamically metastable but can occur as part of more complex carbon polymers.

Figure 1 also shows how the different bonding situations are reflected in electron spectroscopy. Depicted are X-ray absorption spectra (XAS) [2] of C_{60} , graphite and diamond (as CVD film [3], with a trace impurity of graphite). The carbon 1s XAS method is chosen as it resolves clearly the presence of delocalised electrons from the π bonds shown in the connectivity diagrams. For oriented surfaces the polarisation dependence of the excitation with synchrotron light allows directly to determine the orientation of the π bond relative to the carbon-carbon backbone bonding which accounts for the high-energy structures. Fullerene and graphite are dissimilar in their spectra mainly because of the molecular character of fullerene giving rise to discrete bands of weakly interacting molecular orbitals whereas in graphite a complete overlap of molecular states to broad bands of density of states gives only rise to few structures in the spectrum. The ordering of electronic states with energy is, however, very similar for the two carbons with the same connectivity.

2.1.10.4. The Basic Structures

The two allotropes of carbon with particularly well defined properties are hexagonal graphite, as thermodynamically stable modification at ambient conditions, and its high-pressure, high temperature allotrope, cubic diamond. Although both well-crystallised forms will only very rarely be encountered in catalytic systems it is important to recall some details about their properties as they prevail also in the practical forms of carbon.

The idealised crystal structures are displayed in Figure 2. The consequences of the different connectivities can clearly be seen. Diamond is an isotropic material consisting of corner-sharing tetrahedra equivalent to a face-centred close-packed structure of carbon atoms with additional atoms in the centres of every other octant of the cubic unit cell. The ideal tetrahedral arrangement of carbon atoms leads to four equal bonds of 154 pm length. The long-range ordering can be described by layers of bent carbon hexagons with one additional interlayer bond per carbon atoms. The bent hexagons are equivalent to cyclohexane with the in-plane bonds in equatorial and the interlayer bonds in axial positions. The resulting crystals are highly symmetric (space group $Fd3m$) with a preferred (111) cleavage plane. One finds in the literature a historic classification of diamond according to their optical absorption properties which are predominantly controlled by the abundance of substitutional nitrogen and boron atoms.

The structural properties are reflected in the physical properties selected in Table 1. Diamond is a superhard, electrical insulator with an extremely good thermal conductivity. Phase transitions into the liquid state or sublimation occur outside the range of conditions in catalysis (see Table 1). Its chemical reactivity is very

limited, occurring mainly through a catalysed transformation into graphite. From there oxidation and halogenation reactions will occur. An extensive report about structural, morphological and kinetic aspects can be found in the literature [4].

Table 1: Selected Properties of Hexagonal Graphite and Cubic Diamond

Property	Graphite	Diamond
Density (g/cm^3)	2.266	3.514
C-C bond length (pm)	142	154
Enthalpy of sublimation (kJ/mol)	715	710
Enthalpy of oxidation (kJ/mol)	393.51	395.41
Enthalpy of formation (kJ/mol)	0.0	1.90
Melting temperature (K)	2600/ 9 kbar	4100/ 125 kbar
Thermal expansion (1/K)	$-1 \times 10^{-6} / +29 \times 10^{-6}$	1×10^{-6}
Electrical resistivity (Ω/cm)	$5 \times 10^{-7} / 1$	10^{20}
Mohs hardness	0.5 / 9	10

Anisotropic data for graphite are given in directions first parallel to the graphene layers and then perpendicular

The trigonal connectivity leads to a planar arrangement of carbon with stronger bonds between the carbon atoms within the planes as seen from the reduced bond distance of 142 pm. The interplanar distance of 335 pm is significantly larger than the in-plane bonds leading to a significant reduction of the bulk density of graphite as compared to that of diamond (table 1). All physical properties are strongly anisotropic with a metallic character within the plane directions and an insulator behaviour perpendicular to the planes.

The electrical properties (see Table 1) are unusual in that a very small band overlap between valence and conduction band of the order of 0.004 eV allows a very small number of carriers (0.02 electrons per C atom) to move freely with extremely small scattering probability. This yields good electrical in-plane conductivity. Perpendicular to the graphene planes the conductivity is of the zero-band semiconductor type with an inverse temperature coefficient as for the metallic in-plane conductivity. As defects increase in the graphene layers the conduction mechanism gradually changes from metallic to semiconducting with only moderate changes in the absolute resistivity which cannot any longer be measured as an anisotropic quantity. A high density of defect states on both sides of the Fermi level [5] accounts for this behaviour which makes carbon brushes and carbon filament lamps work. The determination of the temperature dependence of the electrical resistivity is a suitable method to determine the degree of graphitic medium range structure in

nanocrystalline carbon materials. It also allows one to follow the structural effects of heat treatment during graphitisation of non-graphitic precursors.

The interplanar bonding forces are of the order of 5 kJ/mole and thus so weak that small changes in electronic structure of adjacent planes allow the swelling of the structure and the incorporation of a very large number of heteroelements and molecular compounds. The electronic changes can either be a weak chemical reduction of the graphene layers by donor compounds such as alkali atoms or a weak oxidation by bromine, halide salts or mineral acids. All these compounds form intercalation structures with complicated structural and physical properties which have been investigated extensively [6].

In ideal graphite the graphene layers are of very large size relative to their thickness and are free of intralayer defects. Furthermore, they are stacked in perfect periodicity either in ABAB or in ABCABC stacking sequences giving rise to hexagonal or rhombohedral graphite. Graphite in catalytic situations is quite far from this structural ideal type. Several types of defects cause the existence of different families of modifications.

Apart from the reactivity towards intercalation, graphite is rather inert to other chemicals except strong oxidising agents which form covalent compounds like graphite fluoride or graphite oxide. Total oxidation of graphite to CO and CO₂ is a highly complex gas-solid reaction which depends sensitively on the defect structure of the graphite. The reason for that is the chemical inertness of the ideal graphene layer which cannot be attacked by molecular or atomic oxygen at thermal energies. Reaction occurs thus only at defects like missing atoms, or non-hexagons and on the perimeter of the graphene layer which collectively form the prism faces of graphite crystal. As these faces are a strong minority of the order of below 0.1% frequency in the face distribution of the graphite crystals (platelet habitus) the number of reactive centres for oxidation is small in graphite. The reactivity depends thus heavily on the additional sites provided by in-plane defects.

In summary, graphite and diamond are two modifications of carbon with similar strong bonds between the carbon atoms (difference in bond length 8.5%). The differing hybridisation leads to a different dimensionality of the covalent interaction. A strong structural anisotropy for graphite as compared to a perfectly isotropic diamond structure causes a series of fundamental physical and structural differences. The differing strengths in the carbon-carbon bonding provide the handle to discriminate with a variety of spectroscopic methods (see Figure 1) the two modifications. Such methods are of minor importance as long as crystalline materials are under discussion. In catalytic situations, however, multi-phase amorphous carbon is frequently encountered which cannot be analysed convincingly with diffraction techniques.

The modifications of fullerenes and carbiners which are also well-defined forms of carbon are, however, very rare in their pure forms in catalytic materials. For this reason they will not be treated in detail in this work.

Briefly, carbiners are molecular crystals of columns of carbon atoms linked with alternating single and triple bonds. The column length seems variable but mass-spectral data suggest frequent lengths between 10 and 20 carbon atoms. A collection of properties of these silver-white carbons prepared from shock sublimation of graphite which seem stable only at temperatures above 2300 K but survive storage in natural conditions for thousands of years can be found in the literature [7].

Fullerenes [8,9] are a large family of molecular carbon which do not contain heteroatoms as in organic molecules. They form cage structures with all carbon atoms in the sp² configuration. The three-dimensional structure is made possible by a controlled incorporation of pentagons [8] into the hexagon network. The high symmetry of the resulting ball-shaped molecules is the consequence of certain rules of combinations such as never combining two pentagons and including only 12 pentagons in every molecule. In the frequent case of not following these rules the bent carbon sheets polymerise to form complex amorphous carbons called fullerene black [10]. It is very important, for the present context, to notice that the chemistry of these spherical sp² carbons is substantially different from that of planar-allotrope graphite. The distinction arises from the strain in the weak bonds of the fullerenes. The non-planar geometry of the backbone reduces the orbital overlap of the pi-electrons (see Figure 1) causing localisation of the double bonds and an overall chemistry of an electron-poor electrophilic poly-olefine [11,12,13]. One consequence of this is an enhanced reactivity of fullerenes against oxygen compared to graphite [13,14,15]. Bends in graphene layers are thus preferred centres of chemical reactivity even without the existence of a co-ordinative undersaturation.

2.1.10.5. The Less Well-Defined Structures

Figure 3 summarises some families of carbon materials which are defective variants of the basic allotropes shown in the top line of the scheme. These materials exhibit distinctly different properties compared to the idealised, parent structures so that they are often considered as carbon modifications on their own. In the bottom lines the long range ordering types and the crystal types are given for the families of materials.

Carbolites [7] are orange coloured transparent solids with a very low density of 1.46 g/cm³. They can be prepared by graphite evaporation under conditions similar to fullerene formation using , however, argon or argon/hydrogen as quench gas at higher pressures than suitable for fullerene formation. The structural properties are collected in Table 2. The structural models of short chains of carbine structure with assumed interchain cross-links is controversial. The material is rather stable in ambient conditions. High-temperature processes and high temperature gradients are pre-requisites for their formation.

The fullerenes [9,8,16] are well-defined molecular solids for the smallest compounds mainly for

C₆₀, C₇₀, C₇₂ and C₈₄ which can be obtained in measurable quantities as purified materials. These molecules are soluble in solvents such as toluene or trichlorobenzene. They form deeply coloured solutions which can be purified by liquid phase chromatography. The respective molecular solid needs careful sublimation to remove solvent and gas adducts. Fullerenes are air-sensitive [17] and light-sensitive [11] and decompose slowly under polymerisation (becoming insoluble after storage of day in air).

Table 2: Structural Characteristic Data for Various Carbon Forms

Unit Cell Parameters

Carbon	a - axis (pm)	c - axis (pm)	γ (deg)
graphite hexagonal	246.2	676.8	120
carbine	894.0	1536.0	120
carbine II	824.0	768.0	120
carbolite	11928	1062	120
diamond cubic	356.7	---	---

Raman Frequencies in cm⁻¹

graphite	1582	sharp
diamond	1332	sharp
carbon black	1355	broad
a-CH	1332 + 1500	sharp + broad
glassy carbon	1359 + 1600	broad + broad
nanotubes (mixtures)	1566 + 1592	sharp + sharp

The large number of predicted larger molecular structures [18] have not been observed as pure compounds although evidence for the formation of larger cage molecules comes from TEM investigations of the residues of evaporated graphite after extraction of the small soluble fullerenes [19]. Such cage molecules may be present in many amorphous carbon materials which have been subjected to high enough temperatures required for the skeletal rearrangement. These temperatures are reached in many combustion processes and in understoichiometric oxidation reactions of aromatic and aliphatic hydrocarbons as was shown by mass spectrometric studies [20]. These studies show that fullerenes can occur in many conventional reactions and not only in graphite evaporation processes which are not frequent in catalytic chemistry.

A class of intermediate compounds between graphite and fullerenes are the nanotube materials. Nanotubes are a special subgroup of graphite fibre materials [21] which can be formed in a wide variety of structural elements. Nanotubes consist of helical twisted [22] sheets of graphite capped with two half-shells of molecular fullerenes. This continuous arrangement of sp²

carbons exhibits very special electronic properties [23] and is a highly desirable material which is still difficult to obtain in the pure form. Nanotubes frequently contain several layers of graphene sheets wrapped concentrically around each other. In catalytic chemistry this form of tubes or filaments is rather rare. They are very much in contrast to other forms of carbon filaments or tubes which are created under the influence of catalytic conversion of hydrocarbons (see below). Figure 4 summarises common forms of graphitic filaments [24] which all consist of graphene sheets which are stacked together without chemical bonds between the basic structural units (BSU) [25]. This lack of continuous chemical bonding drastically affects the electronic properties and the chemical reactivity which are comparable to that of planar graphite. The dark blocks in Figure 4 symbolise the location of the catalyst which is most effective when it contains iron or nickel. The combination of catalytic metals like iron or nickel with impurities like phosphanes leads to the growth of extremely unusual forms of carbon fibres such as helically wound graphite spirals from acetylene at 975 K [26]. Under catalytic conditions a wide variety of carbon filaments which may not be linear but resemble “spaghetti piles” are possible and may not be recognised as carbon. This is illustrated in Figure 4 with a silver catalyst used for methanol dehydrogenation with a deposit as spaghetti pile. The identification of carbon was possible by selective area electron diffraction and by energy-dispersive X-ray analysis. From the diffraction pattern it occurs that the internal structure of the fibres is as displayed in the top left schematic drawing.

Onion carbon [27] is also a derivative of graphite which is made from concentric spherical graphene layers which are said to be continuous [28]. A more frequent form of polyhedral graphite particles is made from packages of concentric graphene layers which are bent but not closed by continuous chemical bonds. Such materials occur in graphitisation processes of all kinds of precursors and can grow into sizes of several microns. As it was not possible to isolate mg amounts of onion carbon little is known about their chemical properties. Their existence in any carbon material indicates, however, a thermal prehistory of graphitisation conditions meaning temperatures well above 1500 K with reducing or inert gas phase compositions.

A large group of carbon materials represent the disorder varieties of graphite. Figure 5 summarises stacking schemes along the crystallographic c-axis. Scheme 5A shows the stacking of large graphene layers which can be continuous up to lateral sizes of several hundred micrometers. The most frequently observed regular stacking of carbon atoms within the sheets are the hexagonal ABA stacking and in natural graphite and the rhombohedral ABCA stacking. Regular stacking of the graphene layers which are only very weakly bound toward each other (by induced dipole moments of the “aromatic” π electrons) is given by a closest packing of the carbon atom spheres giving rise to the following dimensions for ideal hexagonal graphite:

in-plane distance 142.1 pm
 in-plane lattice constant 246.2 pm
 c-axis lattice constant 670.8 pm
 interlayer distance 353.9 pm

The rhombohedral graphite polymorph is slightly less stable than hexagonal graphite and converts during oxidation or even during mechanical treatment (ultrasonication, milling) into the hexagonal form. It can be discriminated by its powder X-ray diffractogram in the region of the “cross lattice reflections ($h \neq 0, l \neq 0$)” which are generally sensitive to stacking order of a graphite material. The presence of rhombohedral reflections can be used as an absolute criterion to identify natural graphite.

As the interlayer bonding in graphite is so weak, it is easily possible to obtain graphite with little or no regular stacking order which results in the extreme difficulty of obtaining single crystals of graphite. The interlayer distance increases up to 344 pm as a consequence of the absence of stacking. Even higher values are sometimes found in the literature which are characteristic for nanocrystalline carbon in which the graphene layers are no longer parallel to each other (see Figure 15). A large number of graphitic materials exists between these two cases in which the graphene layers become successively smaller and form packages of parallel layer fragments named as basic structural units. These packages can either be aligned in parallel or may be inclined towards each other. In Figure 5B regular arrays of parallel and inclined stacks of BSU can be seen. This alignment is characteristic of synthetic graphite used as catalyst support materials. As the chemistry of the edges of the BSU stacks is very different from that of the basal planes one observes a patterned surface chemistry. The patterning depends in its contrast on the average angle of inclination. In synthetic graphite which is post-annealed after its formation under high temperature and at hydrostatic pressure [29] (highly oriented pyrolytic graphite, HOPG, see Figure 3) this angle is as low as 1 degree for top quality samples used as graphite monochromators. At angles above 5 degrees up to 30 degrees one refers to the materials as pyrographite. The absence of any preferential alignment is observed between the BSU stacks in pyrocarbons and some carbon black materials. Such a secondary structure is often observed when the process of carbon generation occurs at low temperatures or in large temperature gradients. The surface chemistry of these hard carbons is characterised by a hydrophilic nature caused by the many terminating oxygen functionalities on these materials.

Kish graphite is a well-ordered variety of synthetic graphite obtained from exsolution of carbon out of liquid iron. Under certain conditions excess carbon which is insoluble as Fe-C crystallises in a well-ordered platelet morphology which can be isolated by dissolution of the iron matrix in mineral acids. It is the macroscopic variety of the BSU which forms the graphene stacks in filamentous carbon as shown in Figure 4. Under certain cooling conditions of the iron melt these flakes can grow into sizes of 1 mm diameter. They represent by their

extraordinarily high degree of ordering, the closest known approximation to graphite single crystals. In catalytic systems the “micro-kish” graphite particles are also of high crystalline quality rendering them very resistant to chemical transformation in oxidising or reducing atmospheres.

An example of the lateral anisotropy of the surface chemistry resulting from the partial alignment of BSU according to Figure 5B can be seen in Figure 6. The STM wide scan shows a system of trenches in HOPG which was oxidised in air at 1000 K for 30 min. Smooth rectangular stripes of hydrophobic graphitic basal planes coexists with almost the same surface area of prismatic faces of the step surfaces. The wedge-shaped contours are imaging artefacts caused by the STM tip. As oxidation proceeds, mainly on the prismatic edges, a pattern results from high recession velocity in the valleys and a low reactivity at the basal planes.

The unidimensional disorder of graphene stacking has a two-dimensional counterpart in the relative angular orientation of the hexagons within adjacent graphene layers. Figure 7 shows schematically the two possibilities of stacking in two-dimensional registry (relative displacement of carbon atoms 0.5 and 0.5 unit cell lengths, hexagonal stacking) and without registry which is referred to as “turbostratic” disorder. This special state of crystalline disorder is characteristic of layered materials with weak interlayer bonding. Its detection indicates well-developed graphene layers with very little chemical impurities which would force the stacking of layers into a three-dimensional disordered state with no parallel orientation of adjacent BSU. Non-graphitic carbons frequently exhibits this type of disorder with the consequence that all X-ray diffraction peaks other than the (002) line are absent or very broad.

These disordered carbons constitute a transition form between graphite and carbon blacks which are turbostratic materials with the additional complication that the lateral size of the BSU becomes very small with typical sizes of below 5 nm. Carbon blacks appear as chain-like aggregates of spherical particles of 10-50 nm diameter [30]. Elemental analysis reveals a significant hydrogen content of $C_{8-12}H$. Such materials are referred to as nanocrystalline carbon as the X-ray diffraction mechanism changes from Bragg diffraction to elastic scattering with the different physics of the scattering process [31,32]. The broad peak in the range of the graphite (002) is no longer a Bragg peak but represents the absolute maximum of the pair correlation function which is dominated by the still parallel arrangement of small graphene layers of sizes comparable to large aromatic hydrocarbons [31].

Figure 8 represents models and high resolution transmission electron microscopy of the secondary structure of carbon blacks forming spherical aggregates. The shell structure of stacks of graphene layers optimises the inter-stack interaction via heteroatoms located at the prism edges of each graphene layer. In many materials the shells are filled by smaller particles or grow around a non-

carbon nucleus. The inter-stack interaction are mediated in many carbon blacks through hydrogen bonds of adjacent OH groups. The outer surface of a black particle also contains significant amounts of OH groups which control the aggregation of the primary spherical particles to fractal larger aggregates, in the literature often called “structure of carbon black”. Modification of the ion strength (in e.g. aqueous solutions) affects the strength of the interaction and influences the aggregation behaviour. Thermal activation of the hydroxyl groups creates dangling bonds and re-orientation of the graphene packages such as to form a covalently cross-linked polymer. The process creates sp^3 bonds and leads to an enormous decrease in chemical reactivity and an increase in mechanical strength. This important aspect of the reactivity of carbons with a high fractional prismatic surface area has the consequence that thermal treatment even under oxidising conditions can transform the reactive carbon black material into highly stable glassy carbon (see below).

Fullerene black is of a similar constitution and secondary structure as normal carbon black with the important difference that its BSU are composed of non-planar graphene layers. Additionally, the stacks are not straight but curved giving rise to a more disordered and less dense carbon material. The chemical reactivity is higher as the stability of non-planar graphene layers is reduced. In addition, the irregular shape of each graphene layer prevents the formation of parallel stacks to a large extent. A fully amorphous array with a large surface fraction of prism faces will result which additionally increase the chemical reactivity.

Figure 9 summarises these interactions in nanocrystalline carbons which constitute a large fraction of carbonaceous deposits on catalytic materials. It is important to note that these carbons exhibit a high reactivity towards polymerisation under weakly oxidising conditions (inert, vacuum steam, reducing) and a high reactivity towards total oxidation under strongly oxidising conditions. Both reactivity patterns are a consequence of the high ratio of prismatic to basal surface area of the carbon stacks. The materials in Figure 9 A,B result from weak interactions between the various building blocks. A carbon with sp^2 and sp^3 local bond geometries is formed after polymerisation by cross linking with bonds, atoms or even molecules as schematically illustrated in Figure 9C.

The resulting hard carbon black is non-graphitisable by thermal treatment up to 3000 K. The sp^3 bond cannot be re-hybridised to sp^2 . These hard carbons are often referred to in catalytic systems as carbonaceous deposit. The material contains some heteroatoms (usually hydrogen). It is chemically heterogeneous, structurally amorphous and mechanically hard and exhibits no graphitic properties, although the large majority of all carbon-carbon bonds are sp^2 hybridised. Higher contents of heteroatoms and the presence of nitrogen, sulphur and oxygen are characteristic properties of coke, the product from carbonisation of coal or other hydrocarbon sources with larger molecular constituents. Carbonisation is a

polymerisation process in which small molecules like methane are liberated. Heteroatoms in the form of ammonia, water and hydrogen disulphide are removed and irregular stacks of small graphene layers (originating from the large organic molecules) are cross-linked by molecular fragments under preservation of the irregular orientation of the stacks (see Figure 9C).

In a-CH or diamond-like carbon (DLC) the hydrogen content is as high as $CH_{0.4}$ and the carbon atoms are arranged in ribbons or chains with no discernible stack structure of graphene layers. Glassy carbon is a technical product made from carbonisation of organic polymers and consists of ribbons of sp^2 carbon with a significant contribution of non-hexagonal rings allowing a three-dimensional tangled structure. This creates the high mechanical hardness and the resistance against graphitisation lending this material excellent mechanical stability at high thermal and mechanical load (only under non-oxidising conditions). Turbostratic stacks of 3 nm width and 10 nm length form the continuously bent BSU of this carbon which can be formed in catalytic reactions allowing polymerisation of molecular precursors followed by carbonisation at around 1000 K (in regeneration cycles for example). The content of sp^3 bonds is low in this material but the hydrogen content is significant which is required to saturate the high specific prismatic surface area of the ribbons.

Active carbon or charcoal is an important modification of carbon in catalysis. It consists of carbonised biopolymer material which is in a second step activated. This procedure creates a high specific surface area by oxidative generation of micropores of very variable size and shape distribution. A more controlled activation is achieved by the addition of phosphoric acid or zinc chloride to the raw product. The additive is incorporated during carbonisation into the hard carbon and is subsequently removed by leaching creating the empty voids in a more narrow pore size distribution as achievable by oxidation. Other activation strategies employ liquid oxidants such as nitric acid to create large pores with a very wide size distribution. Today, several thousands of patents describe numerous ways to structurally activate carbon [33] from mostly natural sources.

A large number of oxygen functional groups are created during the activation process by saturation of dangling bonds with oxygen. This creates a rich surface chemistry which is used for selective adsorption. In addition, it determines the ion exchange properties which are relevant for catalyst loading with active components. A more detailed description of the surface chemical aspects which are most relevant for the catalytic uses of nanocrystalline and activated carbons follows below. The microstructure of activated carbon may be described by the archetypes depicted in Figure 9B and 9C and may even contain significant amounts of graphitic structure [34] depending on the temperature regime of activation. The micromorphology is often characteristic of the biological origin of the raw material with shapes of cell arrays and

even whole plant organs being detectable by SEM imaging. Active carbon contains significant amounts of inorganic matter (iron silicates, silicates, calcium oxides etc.) which is analysed as ash content after complete combustion. Activated carbons are very heterogeneous materials and are difficult to characterise in microstructure and reactivity. Recent reviews about this class of large scale technical carbons can be found in the literature [35, 36].

To summarise, a wide variety of forms of carbon can be found under catalytic conditions. In particular, during deposition and thermal post-treatments a very complex carbon material with unexpected chemical and structural properties can result causing severe problems in catalyst regeneration and modification of its properties during de-activation. The group of carbons which are used deliberately in catalytic systems is summarised in Table 3 together with its most important physical parameter, the specific geometric surface area. The values vary over 3 decades and reach values between geometric surfaces of micron- size particles up to the surface area of the number of carbon atoms in the sample. This latter values are

Table 3: Different Types of Carbon Supports with Ranges of Geometric Surface Areas in m²/g

Carbon	Surface Area
Natural graphite	0.1 - 20
Synthetic graphite	0.3 - 300
Graphitised carbon blacks	20 - 150
Carbon blacks	40 - 250
Activated carbon from wood	300 - 1000
Activated carbon from peat	400 - 1200
Activated carbon from coal (coke)	200 - 1000
Activated carbon from coconut shells	700 - 1500

unphysical if they are interpreted in terms of a monolayer coverage of the nitrogen probe molecules. Highly porous carbons exhibit pronounced capillary condensation phenomena requiring a full BET isothermal analysis for the determination of the true geometric surface area. Although this is widely known and described in detail in other sections of this handbook, it is still customary to present these very high numbers of “BET surface area”. Care must be taken in comparing data based on surface area measurements in carbon chemistry as some sources determine the monolayer sorption capacity whereas many other sources do not. For this reason also surface area values determined with various adsorbents like nitrogen, CO₂ or Kr may differ significantly as these probe molecules exhibit quite different condensation properties at the conditions of adsorption. The most useful contribution of sorption data to evaluate the nature and size distribution of porosity in carbon materials will not be discussed here.

It is noted that in different areas the use of terminology to describe structure and properties of carbons is quite different. Within the carbon -science community a clear system of terminology and definitions was elaborated which is recommended to be used whenever applicable. A listing of this definitions can be found in the literature [37,38].

2.1.10.6. Formation of Carbon Materials, General Pathways

The technical synthesis of graphite, diamond and a variety of other forms of sp² carbons (Figure 3) is described in a review [39] and will not be covered here. As the unintended formation of carbon in deactivation processes and the modification of primary carbon surfaces during chemical treatment (in catalytic service and during oxidative reactivating) in their chemical properties are frequent problems encountered in catalytic carbon chemistry, it seems appropriate to discuss some general mechanistic ideas which mostly stem from the analysis of homogeneous combustion processes (flame chemistry) and from controlled-atmosphere electron microscopy.

The source of all carbon relevant in the present context is a feedstock of hydrocarbon molecules (aliphatic, aromatic, with and without heteroatoms). Figure 10 summarises the possibilities of its conversion into black carbon. The “chemical” route comprises polymerisation into aromatic hydrocarbons with final thermal dehydrogenation. This process often includes a liquid crystalline phase immediately before final solidification. In this phase large aromatic molecules can self organise to parallel stacks and so form well-ordered precursors for graphitic structures with large planar graphene layers. This phase is referred to as mesophase and can be observed by polarised light optical microscopy.

The “physical” pathway requires activation of the molecules by high external energy input such as high-temperature flames, projectiles like accelerated and free electrons or the presence of a plasma source. Such conditions can also occur in analytical instruments like electron spectrometers and microscopes which have a potential to create black carbon during analytical inspection of hydrocarbon layers [27]. In all these cases the molecules are fragmented and dehydrogenated in one process and represent a source of free carbon atoms or small fragments like C₂ dimers. These fragments condense into chains of carbon atoms which have a strong tendency to form small ring molecules by nucleophilic self-substitution of the end groups. Saturation of the dangling bonds of the primary rings by polymerisation leads to graphene layers. These processes occur very rapidly compared to the slow activation along the “chemical” path. Little time is available for orientation of the rings into stacks and cross-linking into non-planar units can easily occur (see Figure 9). Hard, non-graphitisable carbons are the final products of these processes in which all fullerenes and fullerene blacks are also formed.

A large number of intermediate pathways are possible when catalytic reactions interfere with the polymerisation/dehydrogenation steps. A common scenario is the catalytic dehydrogenation of hydrocarbons on nickel surfaces followed by dissolution of the activated carbon atoms and exsolution of graphene layers after exceeding the solubility limit of carbon in nickel. Such processes were observed experimentally [40] and were used to explain the shapes of carbon filaments. In the most recent synthetic routes to nanotubes [41] the catalytic action of in-situ prepared iron metal particles was applied to create a catalyst for dehydrogenation of either ethylene or benzene.

2.1.10.7. Formation of Carbon Materials, Mechanistic Aspects

A schematic correlation between reaction pathways and principal structural properties of common carbon forms according to the classifications in Figure 3 is presented in Figure 11. The literature [33] is rather controversial [42] allowing only a survey of chemically plausible pathways relevant for the present conditions of possible carbon formation.

Three main synthetic routes to carbon can be identified. None of these routes produces exclusively one phase or modification of carbon. In all cases, mixtures of carbons are always produced as indicated by the central box in Figure 11. This complexity highlights the generally strong influence of kinetic aspects in the formation reactions. The realisation of a perfect sp^2 local configuration is always energetically favourable and is reached in graphene layers with only hexagonal constituents. The saturation of the peripheral dangling bonds of graphenes can occur either by homonuclear cross-linking resulting in macroscopic planes, irregular arrays of stacked graphenes, or by heteronuclear bonding resulting in either polymers or surface functional groups. Metastable configurations contain mixtures of six-membered rings with other ring geometries causing strain in the sp^2 bonds. Non-planar structures of a wide variety result. These structures are chemically highly reactive and disappear in oxidising or hydrogenating atmospheres preferentially over planar structures. This explains an additional strong influence of the gas phase conditions on the distribution of carbon materials

The group of synthesis routes at the top of Figure 11 combines the chemistry of carbon formation in combustion processes. This chemistry is summarised in two reviews [43,42]. In high-temperature combustion reactions (above 1200 K) the general reaction occurs via the “physical” pathway indicated in Figure 10 with initial fragmentation into neutrals and thermo-ions (without an additional source of energy). C₂ fragments such as acetylene, or oligomers react to carbon chains which form predominantly aromatic molecular fragments (with dangling bonds) and to a lesser extent in combustion atmospheres three-dimensional cage structures with both sp^2 and sp^3 bonds (becoming a dominant path in fullerene-

generating conditions). In co-operation with ionic fragments these secondary building blocks condense to the graphene BSU with planar or bent layer structure. In a detailed analysis of the flame chemistry [44,45,46] a three zone model of a flame was derived. The elementary building blocks for carbon are formed in the hottest oxidation zone. A surrounding zone with luminous constituents is identified as the location of chain growth into poly-acetylene molecules of the form C_nH₂. In the third dark zone these molecules rearrange into polycyclic hydrocarbons and finally into graphene layers. Ample evidence for this model came from mass spectral analysis of the gasphase in various types of flames. It needs to be pointed out that this diagnostic method gives no indication about the reactive particles as by the time of their detection they are energetically cold and represent the ground state of a mere spectator species rather than the reaction intermediate. For this reason it is difficult to see that long linear chains should be important intermediates as they are never found in carbon products. A scenario in which these processes are modified by interaction of thermo-ions [47,48] and/or aromatic radicals [49] and several independent repair mechanisms for a maximum yield of six-membered condensed rings is more plausible [42]. The kinetic boundary conditions are of great importance in all these processes as large local temperature gradients are required to allow a significant accumulation of carbons from reactive intermediates. At constant high temperatures the unstable species decomposes effectively back into its constituents. This was studied in detail in several types of combustion reactions [45] and is the guiding principle of all technical processes for carbon black synthesis [39].

Another important aspect is the nature of the hydrocarbon source in relation to the efficiency of carbon formation. The idea that the structure of the molecule should be relevant for the carbon formation (aromatic molecules are better than aliphatic structures) is incorrect in all situations where a pool of primary building blocks is formed (in flames, under oxidative polymerisation conditions and under physical activation). Correct is, however, that a decrease in the average C-C bond energy allows easier chemical fragmentation and enhances thus the rate of carbon formation [50].

The growth of carbon particles cannot occur in one synthetic step by condensation of small molecular units. However large an aromatic molecule may grow [47,48,49] it will be too small to create a micron size carbon particle. Three major routes can lead to such large particles: The most unlikely case is a continuous polymerisation process at the “surface” of a fullerene molecule [8]. Both the unfavourable kinetics [51] and the absence of structural evidence that fullerene-like structural elements (characteristic C-C bond lengths) occur in the radial distribution function of black carbon material [31] are strong indicators that carbon particles although of spherical morphology grow in a heterogeneous rather than in a homogeneous way. In a combined kinetic, statistical and microscopic analysis of the growth process [47, 52] the

model of surface growth was put forward. According to this, the poly-aromatic molecules are dehydrogenated and the dangling bonds are saturated by co-condensation of acetylene units. A mass growth of carbon particles of 90% of the total carbon inventory could be explained in this way which is in excellent agreement with experimental flame studies [47]. The prediction of this model of a structureless agglomerate of aromatic molecules surrounded by a concentric array of graphene layers [52] is in excellent agreement with all HRTEM observations of homogeneously produced carbon particles. The spherical texture is assumed to be the consequence of a “droplet” formation of aromatic molecules in the initial stages of carbon fragment supersaturation required for homogeneous nucleation. These droplets are not residues from the possible liquid initial fuel but occur as a consequence of the very rapid initial polymerisation of the highly active small carbon fragments.

In summary, all processes which homogeneously generate carbon from molecular precursors and from homogeneous activation lead to spherical particles made from graphene layers (see Figures 8, 9B, 9C). Spontaneous growth from supersaturated reservoirs of small molecular precursors (chains, acetylene structures, poly-acetylenes) of PAH and co-condensation with smaller molecular fragments lead to spherical carbon particles which aggregate to chains of spheres.

Carbons with much larger continuous graphene layers can be obtained from pyrolytic polymerisation of pre-polymerised hydrocarbons. Synthetic materials like kapton or poly-acrylo-nitrile (PAN) or biopolymers such as coconut shells, wood coal, rice husks and similar materials can be used. Carbonisation or “coking” involves the chemical removal of all heteroatoms such as nitrogen or sulphur and the cross-linking of the polymeric blocks via the dangling bonds created by the removal of the heteroatoms. In this way the texture of the precursor material is preserved in the final product. As no fragmentation of the precursor is required, this way of carbon generation is much less energy-intensive. It further leads to a great variety of structural properties with extreme examples as shown in Figure 9. The possibility to retain part of the heteroatoms such as silicates in biomass carbon makes it possible to obtain extra strong carbons (silicate reinforced) which in addition can be useful for anchoring catalytically active metal components such as noble metal particles. The exact chemistry of carbonisation is complex and depends on the nature of the precursor and on the gas phase chosen (inert, oxidising, steam, reducing). For this reason no general description of this difficult to control process is possible which occurs between 500 K and 1000 K.

2.1.10.8. Catalytic Formation of Carbon from Molecules

The catalytic generation of carbon (Figure 11, left side) is of significant relevance as deactivation reaction in many

catalytic processes involve the presence of hydrocarbons and transition metal reaction sites which catalyse dehydrogenation reactions or solid acid-base centres catalysing polymerisation reactions (see Figure 10). In a review [24] a large amount of kinetic data was compiled about the type of carbon deposited as a function of deposition temperature. The representation in Figure 12 shows that the predominant carbon form is filamentous carbon at most catalytically useful temperatures. The carbon source may be CO or methane, acetylene or other hydrocarbons. The metals for which this correlation is valid are either nickel or iron on all kinds of conventional supports and also as binary or Cu alloys. It is important to note that forms of carbon other than filaments almost do not grow under the conditions of for example steam reforming or Fischer-Tropsch synthesis conditions.

The sequence of events of growth of these filaments which can destroy the whole catalyst bed is now well understood and is presented as summary of several fundamental articles [53,54,55,56]. Electron micrographs of catalyst particles show that they are detached from their support and form either the front or occasionally the centre of a growing carbon filament. In all cases the shape of the particle changes during operation as filament growth catalyst. The growth of an anisotropic carbon particle requires structure-sensitivity of the process of carbon atom-to-graphite polymerisation. Otherwise a shell of graphite would be produced around a core of metal which would stop to act as catalysts after completion of the carbon shell. Such morphologies are also observed but will not be discussed here as they occur either at high temperatures (see Figure 12) or under unusual gas phase conditions which are lean in carbon sources. The fact that very little amorphous carbon with uncontrolled polymerisation of the BSU is produced further illustrates the relevance of the metal catalyst particle which not only generates the source for the solid carbon formation but also controls the geometry of the polymerisation process.

The structure-sensitivity of the catalyst is induced in an induction period in which carbon is dissolved into the metal. A flat surface with a sub-surface carbide forms which dissociates the molecular carbon source. The activated atoms diffuse through this layer and migrate to other faces where they exsolve forming graphene layers. The reconstruction was observed by electron microscopy revealing a deformation of spherical metal particles into droplet-like conical particles. The base forms the active surface for dissociative adsorption and is always directed away from the surface from which the filament grows. The conical mantels are faceted in various directions and allow the growth of graphene layers with different velocities with different orientation. This allows the structures of Figure 4 to result from different abundancies of different facet orientations. Co-adsorption of impurities like oxygen or sulphur affect strongly the growth kinetics by affecting the reconstruction. This sensitivity of the carbon generation process on surface orientation can be used advantageously by controlling shape and rate of carbon filament growth.

Inhibition as well as enhanced production of carbon filaments can be achieved. Additives in the gas phase (oxygen, sulphides, phosphorous compounds) or the promotion with alkali or boron oxide affect the metal facetting. Additives of alloys like molybdenum, silicon or tungsten influence the migration kinetics and the thermodynamic solubility limits of the carbon atoms in the metal particles (10 - 300 nm diameter) which is often believed to be the rate-limiting step in the overall process. A number of models differ in the character of the carbide phase which can be a solid solution or a well-detectable phase like cementite in the Fe-C system. An additional source of discrepancy is the origin of the carbon concentration gradient allowing continuous transport through the metal particle. Thermal gradients were excluded by several independent experiment and convincing circumstantial evidence.

2.1.10.9. Carbon on Noble Metal Catalysts

In catalytic reactions of hydrocarbon conversions on noble metals (hydrogenation, isomerisations over platinum or rhodium as typical examples) it was found that sub-monolayer quantities of carbonaceous deposits exert a dominating influence on the sequence of events. This is also known in practical applications where it is noted that a little “pre-reaction” time in hydrocarbon atmosphere is required to obtain a selective performance. The beneficial effect of the carbon overlayer is believed to arise from a moderation of the de-hydrogenation activity of noble metal surfaces. Dehydrogenation reactions are the fastest reactions catalysed by platinum whereas skeletal rearrangements and hydrogenolysis reactions are about an order of magnitude slower on various single crystal surfaces of platinum at atmospheric pressure and at 573 K [57]. If the hydrocarbon is not adsorbed directly on the metal but is bound instead on a carbon material onto which hydrogen atoms can spill over, it is expected that hydrogenation occurs more selective relative to all other processes. This idea of an intermediate inert surface with intimate contact to the hydrogen-activating metal which was developed during analysis of the “coking” behaviour of supported Ni, Rh, Pd and Pt catalysts [58] requires complete chemical inertness of the carbon against hydrogenation and a suitable electronic structure to permit chemisorption of the organic substrate. In addition, the beneficial effect of structure sensitivity which is prominent in platinum metal catalysis [57] is lost. Combined carbon radiotracer and temperature-programmed desorption experiments on platinum [59] have revealed that up to temperatures of 473 K a carbon species with the composition $C_nH_{1.5n}$ prevails which can be removed in excess hydrogen. At higher exposition temperatures the carbon to hydrogen ratio falls sharply below 1:1 and the resulting carbon is no longer reactive in hydrogen. This more graphitic carbon fulfils the conditions required to act as stable adsorption intermediate. Above 750 K the layer converts into structurally identified graphite which is, however, inactive for hydrogen transfer

as was shown by hydrogen isotopic exchange studies [60]. All reaction carried out with hydrocarbons below 473 K require a permanent re-adsorption of the hydrogen-rich carbon intermediate whereas high-temperature treated platinum is permanently modified and passivated for hydrocarbon reactions above 750 K.

The structure of the hydrogen-poor carbon deposit was not clarified by surface science and is referred to as carbonaceous overlayer. The structural nature of the hydrogen-rich carbon deposit, however, was amenable to a suite of surface science techniques and the unique structure of alkylidines [61] was derived. These adsorbate species which have molecular counterparts in metal organic chemistry [62] consists of at least two carbon atoms one of which is bonded to three metal atoms. The other carbon atoms are fully hydrogenated alkyl groups with only C-C single bonds in-between. On reacting platinum surfaces there is thus no structure sensitivity effect to be expected as a large fraction between 80 at% and 95 at% of all platinum atoms are covered by the carbonaceous deposit which can be of different structure. According to the general scheme of Figure 10 polymerisation and dehydrogenation produce hydrogen-poor molecular species with multiple bonds at the surface. The alkylidine species is a well-defined limiting structure occurring instantaneously on clean metal surfaces [63] upon exposure to pure small alkene molecules. With longer residence time and higher temperature these still hydrogenated species carbonise to result in graphene layers which deactivate the metal surface underneath.

Still controversial [64] is the function of the deposit. It could either act as dynamic cover for non-selective active sites which is compressed laterally upon substrate adsorption and re-expanded after desorption of the product. The alternative function is to serve as weakly interacting surface for the substrate adsorption [65].

One way to clarify the role of the adsorbate is the in-situ investigation of platinum catalysts with electron spectroscopy which is capable of quantitatively determining the abundance and chemical structure of the carbon species present. This has been done for a platinum black [66] material used after various activation procedures in n-hexane conversion reactions. It was found that pristine catalysts are significantly oxidised. These surface oxides are reduced by alkane decomposition into methane, carbon and ethylene. Selectivities to higher hydrocarbons and skeletal isomers of hexane were observed only after an initial induction period. Surface analysis at this stage revealed the presence of Pt metal, of adsorbed OH groups, and a variety of carbon species including carbidic carbon, graphite, amorphous hydrogenated carbon and several partial oxidation products of this polymer. The total abundance of carbon varied between 15 at% for purified Pt and 48 at% after catalysis. The complex situation is summarised in Figure 13. Only a small fraction of the carbon deposit is of a graphitic nature. Most carbon species are still in a state before carbonisation. The nature of the catalytically active stable but reactive carbon deposit may

be a layer of amorphous hydrogenated carbon which is sufficiently stable due to its complex network structure but which is still enough polar to provide active centres for hydrocarbon adsorption.

2.1.10.10. Carbon Formation in Zeolites

Zeolites and other oxide-based solid acid catalysts are used in hydrocarbon conversion reactions with enormous economic impact. Their lifetime is, however, very limited due to deposition of carbon which is referred to in the literature as “coke formation”. The definition of coke in zeolites is very much wider as in the sense of the present article as it is understood that coke is “a carbonaceous deposit which is deficient in hydrogen compared with coke forming molecules” [67]. Two types of coke are discriminated by several techniques amongst which are liquid phase extraction, thermal desorption and spectroscopies like UV-VIS and NMR. The one type is “white coke” which summarises naphthalene-type aromatic molecules including derivatives with alkyl chains and the second type is “black coke” which summarises larger peri-condensed aromatic molecules and alkylated derivatives. This latter type of coke would be referred to in carbon chemistry as a precursor to coke in the sense of Figures 10 and 11.

A significant problem in oxide coke analysis is the determination of the C/H ratio, the most important integral value for a structural characterisation. The main problem is the interference of adsorbed or structural water and the structural change occurring during temperature-programmed analysis allowing for carbonisation and the formation of “irreversible coke” which is structurally identical with black carbon from polymerisation (Figure 11). In a methodical review [67] the solutions to this problem which contributed a lot to the controversial descriptions of coke on oxide catalysts are described in detail. The absence of large amounts of graphitic carbon in zeolite coke was shown recently by using X-ray absorption spectroscopy at the carbon K-edge [68]. The spectra from an industrial zeolite which was treated with aliphatic and complex aromatic hydrocarbon feedstocks to generate coke showed in both cases the predominant presence of cata-condensed aromatic molecules (naphthenes). The independence of the coke properties on the nature of the hydrocarbon feedstock being either methanol (in the MTG process) or small hydrocarbons like ethylene or propylene or aromatic molecules like mesitylene or heavy oil fractions was demonstrated for a technical zeolite sample [69]. This shows that under the influence of the solid acid catalyst the feed is broken into small units from which cata-condensed aromatics (with alkyl side chains or as bridging units) are formed. This process which is similar to the carbon formation in homogeneous systems (flames) occurs at comparatively very low temperatures as low as 475 K. After this polymerisation stage, according to the classification of Figure 10, a step of dehydrogenation up to 700 K follows in which all molecules which can escape the

micropore system react into peri-condensed polycyclic aromatic molecules. All those molecules which remain in the micropores retain their shape and are not polymerised which explains the simultaneous presence of both types of “coke” in zeolites [67]. In subsequent oxidative regeneration steps the peri-condensed molecules at the outer surface carbonise and are eventually oxidised giving free all outer surface according to selective adsorption experiments [69]. The cata-condensed deposits in the micropores cannot fully carbonise due to spatial constraints and remain partly intact as molecular pore blockers reducing the micropore accessibility significantly [69].

The sequence of events in coke formation was studied in model reaction [70] of H-Y zeolite with propene at 723 K. At these drastic conditions the soluble white coke formed rapidly within 20 min and converted into insoluble coke within 6 h of time under inert gas without losing carbon atoms in the deposit. Due to the larger pores in the Y-zeolites compared to the ZSM type zeolites used in the other studies mentioned so far the structure of the aromatic molecules is somewhat different. Soluble coke consisted in this system of alkyl-cyclopenta-pyrenes ($C_{n}H_{2n-26}$, Type A) as hydrogen-rich primary product and of alkyl-benzoperylene ($C_{n}H_{2n-32}$, Type B) and alkyl-coronenes ($C_{n}H_{2n-36}$, Type C) as matured components. The temporal evolution of the various products is presented in Figure 14. It clearly emerges that the soluble coke fractions are precursors for the insoluble coke and that within the soluble coke fraction the final steps of dehydrogenation-polymerisation are very slow compared to the initial formation of smaller aromatic molecules from propene. The sequential formation of precursors with decreasing C to H ratio follows from the shift of the maximum in the abundance of each fraction on the time axis.

The formation of the insoluble coke occurs clearly in several kinetically well discernible stages which can be attributed to initial growth at the outside of the zeolite crystallites and in a slow diffusion-limited growth inside the micropore system. The diffusion limitation will affect the migration of soluble coke molecules rather than the motion of the small precursor molecules. It can be further seen that the acidity of the zeolite is an important controlling parameter which is summarised here rather crudely as the Si to Al ratio. The more acid sites the faster the kinetics and the higher the absolute amount of coke deposition.

The role of the acid sites may be either catalytic or they are consumed irreversibly during coke formation. In the propene “coking” study the abundance of coke molecules remained always significantly below the number of supercages in the zeolite which points together with the fact that insoluble coke formation was not saturated within 30 h on stream to a catalytic function. This was studied in great detail in a combined catalysis FT-IR study [71] which revealed the constant abundance of Brønsted acid sites in modernite with a Si to Al ratio of 12 during coke formation in the ethylbenzene disproportionation. The fact that an IR-active band at 1600 cm^{-1} can be assigned to coke shows

that the structure of zeolite coke is certainly not comparable to coke from coal carbonisation. This was incorrectly supposed in a study of coke formation from hexane and hexene in faujasite zeolites [72]. In this study it was found further that olefinic hydrocarbons are much more active than aliphatic which may, however, be interpreted as inhibition of the initial cleavage of the aliphatic feed molecules which becomes important for long-chain molecules. The ethylbenzene conversion [71] dropped with time on stream and the coke IR band increased proportionally to that without any change in the Brønsted acid band at 3600 cm⁻¹. Moreover, after complete deactivation of ethylbenzene conversion the acid sites were still active for coke formation with a small molecule precursor as ethylene which increased the coke band further when fed after ethylbenzene. This experiment is full in line with the observations from the propene “coking” but remains in conflict with other studies discussed in the literature [67] which either claim the involvement of extremely hygroscopic Lewis acid sites (which are hydrolysed by minute traces of water from hydrocarbon oxidation with lattice oxygen) or the consumption of acid sites during alkene polymerisation (which may be an experimental artefact due to the extreme loss in IR transmittance of the samples in these highly reactive “coking” gas mixtures). It remains an intrinsic disadvantage of this type of studies that IR can only detect various forms of soluble coke (the shifts and varying positions of the coke band are a direct consequence of the successive dehydrogenation-polymerisation of poly-aromatic molecules) and do not indicate the formation, transformation and absolute abundance of insoluble coke which is only detectable in Raman experiments.

2.1.10.11. Graphitisation of Carbons

The various types of carbons obtained by one of the three routes discussed with Figure 11 can be discriminated with respect to their reactivity upon thermal treatment. The lower part of Figure 11 shows the two categories of carbon which will either graphitise (further) upon thermal treatment (annealing) or remain non-graphitic even at temperatures up to 3000 K. The main reason for this distinction of reactivity is the dimensionality of the cross-linking of constituting BSU. If they are linked in three-dimensional networks then little possibility exists by thermal treatment to rearrange the cross-linking into a two-dimensional network which is required to form large planar graphene layers which constitute graphite. The larger the fraction of three-dimensional links in a carbon is, the quicker its formation as there is not sufficient time to reach the equilibrium situation of an all sp² carbon connectivity which excludes three-dimensional networks. Synthesis conditions of rapid quenching from high temperatures are typical for this carbon. Alternatively, the reaction temperature is very low and thus insufficient to provide the activation energy for a re-arrangement of the C-C bonds. In

catalytic situations charcoals and activated carbons are usual materials of this class.

Synthesis conditions of high temperatures with dehydrogenation of hydrocarbons being rate-determining and the intermediate formation of a liquid phase or even a liquid-crystalline phase (mesophase) of two-dimensional stacking of PAH molecules are favourable for reaching the equilibrium situation. Pre-graphitic structures are then formed which require only annealing for better stacking order and polycondensation of the BSU by a final dehydrogenation step. The sequence of events of graphitisation [73] is summarised in Figure 15. The end of the carbonisation process leaves molecular structures consisting of polycyclic aromatic molecules with no heteroatoms other than hydrogen and some alkyl terminating groups. The alignment is parallel to each other as in van-der Waals crystals of polycyclic molecules. The intermolecular dispersive forces between parallel ring systems are responsible for the alignment. At higher temperatures all non-six-membered structures are removed and most of the alkyl groups are removed. At around 1900 K the large aromatic molecules start condensing to graphene layers. As some of the interconnections are not achieved by peri-condensation but by the formation of C-C single bonds considerably strained sheets with significant buckling will result. This state of graphitisation can experimentally be observed by high-resolution TEM [73]. The final step, the “aromatisation” of all C-C bonds occurs only well above 2000 K. Only at such temperatures the parallel alignment of the graphene layers and the formation of a regular stacking occurs as then the abundance of defective structures within the graphene layers becomes small enough to allow the dispersive forces between the graphene layers to direct the orientation of the BSU. These sequences of events with the existence of intermediate stages of ordering between graphite and aromatic molecules has been derived conclusively by X-ray diffraction [74,75]. The evolution of interplanar spacing with carbonisation temperature and the kinetics of its equilibration served as tools for the analysis. The aromatisation was detectable from a shrinking in the a-axis parameter reflecting the shortening of the average C-C bond distance. Both changes lead to a shrinking in the cell volume which is reflected in the relation between the lattice parameters shown in Figure 15. The graphitisation reaction proceeds through a series of “metastable states” [74] with an average change in the carbon-carbon bonding and not via a simple re-orientation of turbostratic units into well-stacked units as it is frequently assumed.

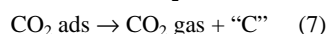
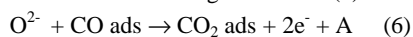
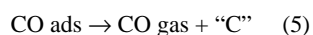
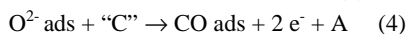
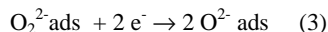
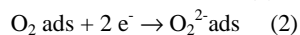
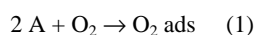
Good candidates for such solid-state phase transformations are carbons produced by polymerisation of pitch, tar or other high boiling fraction of fossil fuels [76]. Pyrocarbons from methane which are generated under conditions of strongly understoichiometric oxidation are also suitable candidates for highly ordered synthetic graphitic materials [29]. In catalytic situations most “carbonaceous deposits”, carbon blacks and synthetic graphite belong to this class of carbons.

The range of temperatures in which graphitisation occurs is between 1100 K and 2500 K with significant variations depending on the number and quality of structural defects in the material. In fullerene material the sequence of events of graphitisation occurs at a temperature level of about 1000 K below that for other carbons [77,78]. The incorporation of large amounts of potential energy in the form of ring tension by the presence of non-six-membered sp^2 carbon rings lowers the activation energy for the solid structural transformations drastically and allows graphitisation at temperatures of e.g. combustion. A similar low-temperature graphitisation is also possible if the carbonaceous deposit on a hydrocarbon catalyst has stored chemical energy in form of highly reactive organic molecular structures.

2.1.10.12. The Reaction of Oxygen with Carbon

This apparently simple reaction is of multiple relevance in catalytic carbon chemistry. The reaction is used to activate carbon by the increase of surface area due to hole burning. It is further used to create surface functional groups (see section 5). Finally it is used to remove undesired carbon deposits in regeneration procedures.

The reaction is a gas/solid interface reaction which requires two independent types [79] of electronically different sites. One site should be electron-rich to activate molecular oxygen (site A), the other site should be electron-deficient to react with activated oxygen atoms (site "C"). A minimal sequence of elementary steps is composed of the following processes:



This sequence of events was suggested by several authors [80,79] with, however, different assignments to the nature of the two sites ranging from "ionic to covalent" [79] to a distribution of sites with varying energy of oxygen chemisorption [81]. In these models it was assumed that the steps (5 to 7) are rate determining.

The steps (1 - 3) designate the activation of molecular oxygen into an oxidising atomic species. This process requires the presence of weakly bound electrons in order to split the di-oxygen double bond. Such "catalytic" sites are available on the basal planes of graphitic carbon. The notion that almost free electrons are also available at structural defect sites [82,83] is only valid for extremely fast reaction rates as otherwise stable surface complexes with oxygen, water or hydrogen deactivate such structural defects. The site A is thus graphene planes with sufficient size to exhibit delocalised electrons more weakly bound than in aromatic molecules [84]. The oxygen atoms will diffuse on the surface [85] using their excess dissociation

energy until they either recombine and desorb or find a structural defect "C" where they can form a covalent bond to carbon (step 4). This reaction is an oxidation reaction in which the directly bonding carbon atom "C" loses two electrons which flow back into the reservoir of almost free electrons of the graphene layer. It is a matter of ongoing debate to decide on the influence of the diffusion of activated oxygen on the overall kinetics [86]. Due to the extremely different reaction conditions and usually intentionally small conversions, at which experiments are made, it is difficult to decide this question at present. The main problem is the integrating effect of the large number of reactive sites present in an oxidising carbon sample which precludes the identification of the influence of any particular reaction step due to the convolution of the elementary step kinetic parameters with the energy distribution of the reactive sites.

The resulting CO complex can either desorb using its energy of formation for activation or survive due to insufficient activation energy. The amount of activation energy depends on the carbon skeleton onto which site "C" is bonded to. It is a structure-sensitive reaction [86,87]. If the primary CO complex remains long enough at the surface where activated oxygen atoms are available (or if a sufficient flux of activated oxygen is available), then complete oxidation will occur according to step (6). The desorption of the oxidation product leaves in any case an empty site for a new attack of an oxygen atom (steps 5,7). The oxidation reactions (steps 4,6) leave an active site each for oxygen adsorption and dissociation. These sites are, however, not those at which the primary oxygen atoms are formed which changed their positions to diffuse from their location of generation on a graphene layer to the oxidation site.

From this scenario which was developed from extensive experimental observations [88,84,89,90,91,92] it is evident that efficient oxidation requires the existence of extended graphene layers for oxygen activation [90,84] and sufficient defect sites for reaction of the activated oxygen. It was found necessary in an extensive formulation of hypothetical elementary steps to invoke the existence of stationary and mobile initial oxidation products (step 4) in order to explain the varying selectivity between CO and CO_2 . The experimental evidence showed different TDS peaks for carbon-oxygen compounds and not for di-oxygen [91,83,93,85] which led the authors to consider only the possibility that reaction products are mobile and not activated oxygen. The process of oxygen activation was assumed to only be possible at the reaction sites themselves ("C" in the reaction scheme). If the activation of molecular oxygen occurs by non-chemical means (glow discharge [83,93] or radiolysis [82]) the sensitivity of the overall reaction kinetics to the presence of graphene layers for oxygen activation is lost and a fully structure-insensitive process occurs. In the other extreme of a di-oxygen reaction on a perfect graphene layer reaction of excessive activated oxygen will always occur at the unavoidable external prism surfaces and very efficiently at the few intralayer defects.

One consequence of the reaction mechanism is that carbon burns with molecular oxygen in a layer-by-layer fashion at a decreasing rate as the perimeter of the graphene stack becomes progressively smaller with increasing burn-off. The defects present in variable abundance in each layer contribute significantly to the rate with an increasing tendency towards burn-off as the perimeter of the etch pits enlarges with ongoing reaction. The resulting net rate is an addition of a constant decreasing term and a fluctuating term with an unpredictable overall behaviour with burn-off. The unusual dominating role of in-plane defects was established by microscopic studies on graphite oxidation [94,95]. This effect precludes a definition of reactivity of carbon materials as their average structure is not sufficiently accurately determined to account for the defect distribution in the carbon which controls the activity. This was established recently [96] for a very wide range of carbons containing most structural features discussed in Figure 3. A “non-linear” compensation effect of the kinetic parameters was discussed. Several groups of carbons with different average structures (graphite, carbon blacks, coals,) are differently affected by the rate-enhancing effect of defects which cause simultaneously a decrease in apparent activation energy and an increase in the pre-exponential factor. The correlation of the kinetic parameters of all carbons results in a non-linear correlation due to the disregarded structural influence.

Alternative reaction scenarios for the activation of the aromatic graphene layers may be considered. A plausible model with a period of increasing defect creation followed by a period of rapid gasification was discarded by in-situ spectroscopic experiments revealing that the average degree of graphitic chemical bonding does not change with burn-off [2]. The local electronic structure of graphitic sp^2 configurations and the extended structural feature of parallel graphene planes is also not drastically changed with burn-off [2]. Disintegration of the well-ordered surface as preparation for oxidation at every surface site, as it was found for the reaction of atomic oxygen [83], is not observed with molecular oxygen.

Recent experiments with in-situ X-ray diffraction [97,99] revealed that defective parts of graphite crystals oxidise preferentially leaving behind a more perfect structure until the total mass loss eliminates the most-well-ordered parts of the crystal. The data are in disagreement with the general experience of solid state chemistry that an increase in defect density creates an increase in gas-solid reactivity. The increase in ordering of the residual graphite surface with progressive oxidation is documented in STM survey images shown in Figure 16. The rough surface of a graphite single crystal [89] which is covered by small crystallites [98] becomes smooth after about 10% burn-off with large terraces and few large step structures indicating the grain boundaries of the crystal. Studies at higher resolution show [99] that the terraces are atomically flat with very few exceptions which are due to certain defects which are more difficult to oxidise than the matrix. A structure with sharp needles and small towers results. These

observations confirm the complex influence of the defects on the oxidation kinetics which can either accelerate or decelerate by various types of defects. Elemental impurities like boron are likely candidates for such inhibiting effects as boron compounds are well known for the inhibiting effect on carbon oxidation [100]. Other known inhibiting groups are C-H and certain C-O surface complexes [101].

The in-situ X-ray diffraction [97,99] data further excluded the possibility that oxygen intercalates between the graphene layers and starts the reaction in a three-dimensional way at the internal surface. Such an in-depth oxidation occurs only at structural defects with three-dimensional character such as grain boundaries and interlayer defects [41,102]. The contribution of this extra-oxidation activity to the overall rate is small but severe consequences arise for the mechanical stability of all carbon materials under oxidative load: At very early stages of oxidation they disintegrate and fall into small particles of individual graphitic crystallites. Such mechanical disintegration has important implications for catalyst support materials where the active component “falls off” at the very beginning of any oxidative load on the system. An extensive review about the uncatalysed and alkali-ion catalysed gasification at defect sites summarises the present status of research in this practically highly relevant area [103].

In any practical consideration of carbon application or intended removal (regeneration) the oxidation reactivity is of importance. Figure 17 summarises results of initial oxidation experiments. Different carbon materials which exhibit all the sp^2 connectivity of carbon atoms exhibit a wide range of oxidation temperatures. The values of these temperatures depend on the definition of reactivity which can be either the first uptake of oxygen, the 50% line of oxygen consumption or even the 50% line of weight loss. Care has to be taken to compare literature values [96,81,104] as all these definitions are in use and the differences in temperatures are quite drastic as can be seen from Figure 17.

The reactivity of the molecular fullerene solid resembles the expected pattern for a homogeneous material. Only a small pre-reactivity at 700 K indicates that a fullerene-oxygen complex [12] is formed as stoichiometric intermediate [15,105] compound. At 723 K the formation of this compound and the complete oxidation are in steady state [12,106,107] with the consequence of a stable rate of oxidation which is nearly independent of the burn-off of the fullerene solid. This solid transforms prior to oxidation into a disordered polymeric material. The process is an example of the alternative reaction scenario sketched above for the graphite oxidation reaction. The simultaneous oxidation of many individual fullerene molecules leaving behind open cages with radical centres is the reason for the polymerisation.

The molecular nature of this carbon allows the spectroscopic identification [15,108] of this intermediate and several oxo-complexes serving as precursor [109,110,105] compounds. On this basis the reactivity of

fullerenes in oxidation is now understood in detail and the reaction scenario is secured by experimental verification [106,111,107].

The other two graphitic carbons oxidise, according to the data in Figure 17, at quite different temperatures and with complex reactivity patterns. They show extensive pre-reaction activity. A significant oxygen consumption initiates at lower temperatures than the main reaction indicating gasification at extra reactive sites. The spread in temperature of this pre-reaction activity is very significant. It has been shown recently that the gasification activity at low temperatures is not a surface effect but can lead to a complete combustion of the whole carbon [112]. This means for practical applications in catalysis that the minimum corrosion temperature of carbon in oxidative atmosphere can be very much lower than the bulk gasification temperature measured by thermogravimetry which is too insensitive in most cases to indicate the pre-reaction activity. The distribution of the pre-reactivity over reaction temperature is not a characteristic property of a carbon material but depends in the same way as the main reactivity on the origin, storage and thermal history of the carbon. The oxidation rate as a function of the geometric carbon surface area (total surface area, TSA) is a sensitive function of extrinsic sample properties [113].

The concept of the existence of an active surface area (ASA) representing a small fraction of the TSA was developed [114] in order to overcome this highly complicated situation. In full analogy to the concept of active sites in catalysis, it was concluded that a surface area measurement with di-oxygen under defined conditions should measure the active sites in combustion ("C" sites in the reaction scheme). This technique allows the detection of the average change of the abundance of active sites with burn-off. The change in ratio between TSA and ASA by over an order of magnitude [114] for a graphitised carbon black highlights the relevance of surface modifications for the oxidation reactivity. A numerical example of the ratio TSA : ASA of 76 m²/g : 0.24 m²/g (ratio 316) at the beginning of burn-off and of 128 m²/g : 2.12 m²/g (ratio 60) at 35 % burn off the graphitised carbon black illustrates the accuracy required to obtain meaningful results. This problem of large ratios may be the reason for the deviating numbers for carbon reactivities still quoted by different authors in the literature [86]. The same concept was further very successful in eliminating all the extrinsic influences on the carbon reactivity over ranges of materials with the consequence that universal rate for the oxidation of sp² carbon was established deviating for various classes of materials only by a factor of about 2 [86, 113].

The method of determination of the ASA creates some carbon-oxygen surface complexes which are non-reactive and causes the still significant dependence of the turn over frequency (TOF) on burn-off or material property. A further improvement of this situation reducing the dependence of the TOF on burn-off to below 10 % was achieved by introducing the concept of reactive surface area (RSA) [86] or active site density [115]. A simultaneous

in-situ measurement of rate and abundance of active sites allows the determination of the RSA without any assumptions on reactivity or energy spread of active sites to be incorporated in the method. The experiment is a transient kinetic measurement as it is well known in catalyst characterisation [116].

The oxidation of carbon can also be catalysed. Two fundamentally different cases should be discriminated. Transition metal oxides and carbides were found to be efficient local sources of atomic oxygen increasing its abundance much above the uncatalysed case. Streams of diffusing oxygen atoms created decorated pathways of non-selective oxidation of basal plane sites as detected by transmission electron microscopy [117,118].

Alkali and earth alkaline metal compounds (hydroxides and bicarbonates) were found to be efficient catalysts reducing the 50% weight loss temperature of all kinds of carbon materials by up to 200 K [103]. Two principally different mode of actions have been proposed for this technologically and scientifically interesting effect. First, it was excluded that alkali graphite intercalation compound could form and modify the surface electronic structure of the top graphene layer to enhance the sticking coefficient of molecular oxygen on carbon. This may, however, result from the action of the strong positive point electrostatic charge of a alkali cation residing chemisorbed at the carbon surface. Oxygen molecules still in the gas phase will become polarised which greatly enhances their sticking probability at the surface. The second effect is related to the set of elementary steps required to form a surface oxygen complex. Many of these structures involve the presence of charged oxygen species which require protons as counterions (carboxylic acids, alcohol, phenols etc.). Alkali ions provide ideal counterions in the situation of gasification where few protons are available. In addition, alkali ions do not only accelerate the formation of salts of surface functional groups but they also cannot act as site blockers like hydrogen which can form very stable surface hydrogen bonds and reduce the number of active sites. Finally, the alkali salts are all strong Brønsted acids which help desorbing acidic surface functional groups to form during carbon oxidation. Using isotope labelling and other kinetic experiments it was established [119,120,121,122] that one very important function in alkali catalysed gasification (with CO₂) is to enhance the amount of exchangeable oxygen between gas phase molecules and surface complexes. A cluster of alkali-oxygen is envisaged as the active species which is loaded with oxygen from the gas phase and unloaded by spillover of oxygen to substrate. A fraction of carbon-oxygen-alkali remains always non-exchangeable which is seen as the "backbone" of the system keeping the alkali at the surface (at high temperatures of about 1000K where evaporation would be a problem) All these effects are discussed in two reviews on the subject [103,123].

A good indicator for the mode of operation of a catalyst in carbon gasification is the ratio of CO and CO₂ which are formed according to the reaction scheme in

independent reactions as simultaneous products. The possible post-oxidation of CO to CO₂ was excluded by a large number of observations and is a basic ingredient in the formulation of the reaction scenario described above. In uncatalysed gasification reactions the product ratio is about unity with a factor of 5 deviations for different carbons. The presence of Ca as catalytic impurities on a carbon from a sooting flame decreased the product ratio to less than 0.01 [81]. A kinetic analysis revealed that the Ca addition enhanced the rate of CO₂ formation without affecting the CO production. The effect was attributed to a modification of the active sites of reaction step (6) which may be envisaged chemically as a Ca salt formation with a suitable surface complex. The suggested analytical value of the CO/CO₂ ratio [81] should, however, be taken with care, as other factors like the basal/prism surface area ratio also affect the product ratio [86,87].

The oxidation of graphitic carbon is a complicated gas-solid interaction with the unusual characteristic of a dependence of the reaction rate on conversion. Several independent factors with different dependencies on conversion co-operate in the control of the overall reaction rate. The most difficult part to control is the strong influence of atomic intralayer defects in the graphitic surface. It was made clear by electron microscopy that these unpredictably occurring reaction initiators can dominate the overall reaction rate [95]. The reaction rate expressed as the normalised mass loss per time as a function of burn-off is schematically shown in Figure 18. In this Figure the main controlling factors and their dependencies on burn-off are indicated. The dominating influence is exerted by the changes in TSA and in fractional active prismatic faces surface area of the graphene stacks. In the initial phase of burn-off the removal of surface defects and surface functional groups determines the rate. This was found experimentally by various techniques [124,89] and is indicated in Figure 16. The initially strongly changing rate leads many researchers to exclude the first 10-20% of the burn-off curve from a kinetic analysis in order not to have to account of this initial effect. For catalytic purposes this effect is highly relevant as the stability of the surface functional groups and surface defects will determine the catalytic reactivity of a carbon sample. In applications where active species are bonded to carbon, the surface structure and its stability determine dispersion and stability of the metal-support system.

All of the effects shown in Figure 18 are accounted for, if the carbon reactivity is given as TOF based on RSA. The only uncontrolled parameter remains the variation in intralayer defect density which is statistical and not measurable by any reaction-based technique (as the technique modifies the number of intralayer defects). This is symbolised in Figure 18 by the wide line for the rate which is a slow function of burn-off and a rapidly varying function of the intralayer defect density.

This information shows that the reactivity of a carbon material relevant in catalysis against oxygen (and other oxidising gases such as CO₂, NO_x, water) is not

easily defined. As almost no experimental studies have ever applied to the RSA-TOF concept it is not surprising that severe inconsistencies about kinetic parameters exist in the literature. A recent review highlights the merits of the transient kinetic technique which is the basis for a unified description of carbon oxidation [125].

The issue of carbon oxidation reactivity is further complicated in all cases where the oxidation of a carbonaceous deposit or a “zeolite coke” is involved. In these cases the solid carbon oxidation kinetics is superimposed on entirely different oxidation pathways involving organic molecules and on the kinetics describing the carbonisation reaction occurring simultaneously with the gasification reaction. The carbonisation reaction system described in Figure 10 is a sequence of polymerisation - dehydrogenation processes which leave essentially pure carbon with widely differing degrees of structural ordering. This carbon which is responsible for the frequently reported conversion from “coke” into “graphite” is not oxidised at moderate temperatures due to the inhibiting effect of the many surface defects precluding oxygen activation.

2.1.10.13. The Surface Chemistry of Carbon

The surface chemistry of carbon is of relevance in all aspects of catalytic carbon chemistry. The two most important heteroelements are hydrogen and oxygen. Each element can undergo a variety of chemically different coordinations which need to be discriminated for analyses of the chemical function of the carbon-heteroatom bond. In the literature the term “surface complex” is often used to describe a group of chemically different bonds which could not be specified in detail.

The local connectivity of surface carbon atoms can be discriminated into sp³, olefinic sp² and aromatic sp² for all kinds of carbon materials of catalytic relevance. Each of the three connectivity can form several types of heterobonds allowing for a broad distribution of carbon heteroatom interactions which co-exist on any surface exhibiting structural defects. The surface chemistry of prismatic and basal planes of sp² carbons is fundamentally different which renders the surface area ratio between the two orientations one of the dominating factors for the description of carbon reactivity. One way of obtaining an estimate about this ratio is to assume that the abundance of hydrophilic sites on a carbon is due to surface functional groups at the prism faces whereas the basal planes should be hydrophobic. The existence of both properties on a carbon can be verified and quantitatively determined by selective chemisorption of long chain aliphatic molecules (n-C₃₂ H₆₆) or metal salts such as H₂AuCl₄ for the hydrophobic sites and alcohol molecules such as n-butanol for the hydrophilic sites. A practical procedure using microcalorimetry has been developed in the literature [126,127].

The complexity of carbon materials together with the surface chemical anisotropy and the modifying effects

of defects creates a highly complex situation for surface chemistry even when only one heteroelement is considered to be actively bonded. It is a characteristic of this branch of chemistry to describe surfaces in terms of distributions of properties rather than in sharp numbers.

The greatest attention in the literature has been paid by far to the carbon-oxygen-hydrogen interaction for their enormous chemical relevance and the existence of a suite of chemical and physical tools for their characterisation. Classes of carbons which are suitable for Table 4: Heteroatoms in Carbon Black Materials

Property	1	2	3	4	5
	Philblack A furnace	Philblack E furnace	Spheron C channel	Spheron 9 channel	Mogul colour
surface area (m ² /g)	45.8	135.1	253.7	115.8	308
total H (g/100gC)	0.35	0.31	0.33	0.62	0.48
total O (g/100 gC)	0.58	1.01	3.14	3.49	8.22
CO ₂ (g/100 gC) *	0.187	0.401	0.575	0.536	2.205
CO (g/100 gC)*	0.343	0.411	2.00	1.928	4.180
H ₂ O (g/100gC)*	0.00	0.435	0.600	0.710	1.440
H ₂ (g/100g C)*	0.209	0.137	0.152	0.321	0.132
H (μmol/m ²)	38.2	11.5	6.5	26.5	7.7
O (μmol/m ²)	7.9	4.7	7.7	18	16.7
CH _x	0.48	0.15	0.08	0.33	0.1
CO _x	0.1	0.06	0.1	0.23	0.21
C _x R	1.72	4.76	5.55	1.79	3.25
ratio H:O	4.8	2.5	0.8	1.43	0.48
ratio CO:CO ₂	1.83	1.02	3.48	3.36	2.04

* integral from thermal desorption up to 1475 K

A representative collection of surface chemical data of several carbon blacks is compiled in Table 4 which was collected from extensive data in a review book [33]. The specific surface area varies over a decade for the five samples. The total content of heteroatoms (determined by classical microanalytical techniques) amounts to between about 1 and 5 wt% which is a sizeable quantity for a material which is nominally pure carbon.

A technique used often in chemical speciation of the surface functional groups is temperature-programmed desorption (TPD) of all functionalities. The strength of the surface chemical bonds requires maximum temperatures of usually 1273 K with desorption profiles extending from 400 K to the upper limit of heating in inert atmosphere in a quartz tube furnace. Table 4 lists the integral abundance of all possible decomposition products of C-O-H functionalities. The data show that both absolute amounts and product distributions (CO to CO₂ ratios) vary significantly and exhibit no apparent correlation to surface area or synthesis method for the carbon. Reduction of the data per surface area reveals that carbon-hydrogen functions are abundant heterobonds on carbon black surfaces. Carbon-oxygen functions are always present and in samples 3 and 5 more frequent than hydrogen terminations. The importance of the heteroatoms for the description of the surface properties becomes apparent

such studies are carbon blacks. These materials are of high elemental purity (no inorganic impurities) and sufficient specific surface area to allow a quantitative determination of the content in heteroelements which is the basis for any meaningful normalisation of surface chemical reactions. In, addition, the spectrum of industrial manufacturing processes [39] and the industrial production allows the comparison of data from homogeneous samples with distinctly different (but often unknown) microstructural properties.

when the carbon to heteroatom ratios are considered. It occurs that about every other carbon atom exhibits in its connectivity one heteroatom. The ratio of carbon to heteroatom can be used to estimate the size of the basic structural units. Assuming the microstructure of carbon to consist of small graphene platelets with few intralayer defects (Figures 5-9) one may estimate from the topology of peri-condensed aromatic structures the ratio carbon to heteroatoms. These are all located at the “prism faces” of the graphene layers and saturate the dangling bonds in the carbon sp² configurations. This ratio is 1.0 for benzene, 1.25 for naphthalene, 1.6 for perylene, 1.76 for coronene and 2.56 for a n = 4 peri-condensed molecule. Such a molecule has a diameter of about 1.2 nm. A coarse correlation between the carbon to heteroatom ratio and the size of a hypothetical circular graphene layer is presented in Figure 19. HRTEM images of carbon blacks exhibit 1.5 - 2.0 nm as characteristic diameters [130] compatible with n = 5-8 ring peri-condensed structures. Samples 2 and 3 from Table 4 exhibit an abundance of heteroatoms consistent with a graphene diameter as seen with physical methods. The other samples consist of significantly smaller BSU which are, however, not observed by microscopy [128,129]. This discrepancy together with the H to O ratio from Table 4 indicates that more than one heteroatom is bound frequently to one peripheral carbon atom calling for

more complex functional group structures than C-H or C=O terminations. Sample 3 is the best approximation to pure carbon in the selection of Table 4 with a large number of simple carbonyl functions as carbon termination groups (see CO to CO₂ ratio). Sample 4 with the lower surface area and the same synthesis history exhibits a much richer surface chemistry which could give rise to a strongly underestimated average size of the graphene layers. It is pointed out here that the physical method of determination of graphene layer diameters by X-ray diffraction [39,33,130] is critical. Smaller particles than the average do not contribute significantly to the overlapping and diffuse line profiles of the (hk) reflections used for the analysis. For this reason it remains valuable to compare physical data with chemical information such as shown in Figure 19.

Using refined X-ray diffraction techniques and the extraction of the radial distribution function from molecular X-ray scattering it was possible recently to develop a model for a graphene layer [31]. This model is free of the difficulties mentioned above and predicts “cluster sizes” between $n = 3$ and $n = 5$ for peri-condensed rings (coronene, hexa-peri-benzo-coronene) in full agreement with electron microscopic [25] and NMR [131] data which led to construction of Figure 19. The model material in [31] was a coal sample before carbonisation containing besides the main fraction of sp^2 centres still about 20 carbon atoms in aliphatic connectivity. This one-dimensional structure analysis represents a real example of the scheme displayed in Figure 9C.

The data from Table 4 show clearly that a significant fraction of the total carbon surface which is chemically active (prism faces and defect sites) is covered by heteroatoms and many of these sites are not just “passivated” by C-H bonds. This situation is also characteristic for carbonaceous deposits with C_xR values of 1.5-2.5 (corresponding C to H ratios 0.45 to 0.65) pointing to truly smaller average diameters of the BSU (see Figure 19) as was determined by chemical extraction and mass spectrometry [70,132,133]. The situation is typical also for carbon materials resulting from dehydrogenation of organic polymers with a large abundance of prism faces and a significant presence of oxygen functional groups. For carbons with larger BSU diameters the dominance of prism sites is gradually reduced and defect sites at crystallite boundaries and intra-plane defects become important locations for surface functional groups. The absolute abundance is, however, so much reduced that the accuracy of elemental analytical data as used above is too low to allow a meaningful chemical and structural interpretation.

2.1.10.14. Non-Oxygen Heteroelements on Carbon Surfaces

The most important heteroelement is hydrogen bound to a variety of different reaction sites. Thermal desorption experiments showed that weakly held hydrogen desorbs at 1000 K, and more strongly bound species desorb at 1270 K and 1470 K. Only above 1900 K all hydrogen is released

from a carbon material [134]. As this extra stable hydrogen can be as much as 30% of all hydrogen present, it was suggested that this species should be bonded to alkene and alkane link-structures within the graphene layers (see Figure 9C) and represent hydrogen bonded to “inner surfaces”.

The chemical structure of the hydrogen groups is difficult to assess as they can be present either directly bonded to carbon or as protons together with other functional groups. In addition, at low temperatures, all hydrophilic carbons carry a layer of molecular water which needs to be desorbed first to allow a quantitative analysis. Thermal desorption with discrimination of water and carbon oxides can be used to control the desorption of the unspecific water layer. It is observed, however, [135,88] that the water desorption affects the surface chemistry of the carbon, as some labile groups are desorbed and the vacant surface sites can react with water to form C-O-H or C-H bonds. IR spectroscopy can be used to show that even after mild desorption of water from an oxidised carbon black a variety of hydrogen species is present at the surface. Figure 20 shows the corresponding transmission spectrum of two technical carbon blacks with hydrophilic and hydrophobic reaction against liquid water after in-situ desorption of molecular water at 573 K: The absorption from carbon-hydrogen and carbon-hydroxyl groups overlap to form a complex peak structure. A range of different O-H groups is present (see below) and the C-H frequencies occur also as convolution of signals from isolated C-H functions and shifted components due to C-H groups next to C-O bonds in various configurations. Figure 20 and the TPD experiments from the literature indicate that hydrogen is present not only in strongly bound C-H groups which co-exists with other functional groups but also in a variety of C-O-H groups which cannot be removed at moderate temperatures up to 675 K. For the hydrophilic sample a broad structure of oligomeric OH group fundamental vibrations causes the strongly falling background at high wavenumbers. After more severe heat treatments the carbon surface is more uniform [136] but is modified in its defect properties and in its chemical reactivity.

The existence of several distinct C-H surface functional groups and the modification of the carbon surface during adsorption of hydrogen has been studied in detail [137]. Four different kinetic regimes of coverage vs. reaction time were identified indicating the structural heterogeneity of the carbon surface. The material studied (graphon) is a graphitised carbon black with no inorganic impurities which allows the deduction at the heterogeneity of the adsorption sites which was also reproduced by a variation in activation energy for adsorption is an intrinsic effect of the carbon material. The fact that temperatures above 700 K are required to saturate the carbon surface allows one to conclude that structural modifications (hydrogen etching) of the surface may significantly contribute to the surface reaction which seems to be more complex than adsorption of hydrogen atoms on (pre-existing) chemisorption sites.

Carbon-nitrogen surface groups are not abundant in carbons made from hydrocarbon precursors. Carbons from nitrogen-containing natural and synthetic polymers contain structural C-N-C groups in aliphatic and aromatic co-ordination. Surface complexes like amines, amides, or nitro groups are not very stable and are desorbed during heat treatment (manufacture, activation, pre-cleaning). An extensive body of work is collected in the literature [135] concerning the intended incorporation of nitrogen from ammonia or cyanides using carbon surfaces pre-reacted with oxygen or halogens. Several structures of C-N and C-N-H have been identified with physical methods. The stability of the most abundant C-N-H groups is, however, rather limited in temperature.

Most significant is the observation that the catalytic behaviour of a carbon (from various sources) remains affected by the amination treatment even when the nitrogen is desorbed from the surface. The explanation was put forward that nitrogen binding (and removal) occurs on defective sites and the nitrogen activation is in fact a mild version of preferential removal of defective surface sites leaving behind a carbon surface with a more graphitic electronic structure than present before. Some of the structural nitrogen (pyridine-like incorporation in the graphene layers) is thermally stable up to 1273 K [33,135] without affecting the catalytic performance of the carbon material. This observation excludes the notion that the heterocyclic substitution injects additional electrons into the conduction band of the semi-metal graphite and in doing so enhances its activity in electron transfer reactions (e.g. activation of molecular oxygen in liquid phase oxidation catalysis [138]).

Carbon-sulphur groups are extremely stable surface compounds which cannot be removed by thermal treatment up to 1470 K. Only by a reductive treatment with hydrogen it is possible to clean carbon from sulphur adsorbates. One source of sulphur is the fuel used for the generation of the carbon from which about 90 % are covalently bonded to the carbon and 10% are segregated as adsorbate which can be removed by solvent extraction. The total amount of sulphur can amount to several wt%. Removal of the structural sulphur is possible by hydrogen reduction to H₂S at about 1000 K. A collection of references on this subject is found in the literature [33]. In activated carbons sulphur can also be present in an oxidised form as sulphate or C-S-O compound.

The generation of sulphur functional groups was investigated in detail in order to prepare anchoring sites on surfaces used in rubber vulcanisation (tire manufacturing). Only those sulphur groups which are not incorporated in the graphene layers can be chemically active for cross-linking polymerisation in vulcanisation. In a broad study, [139] carbon disulphide, hydrogen disulphide, thionyl chloride and sulphur dioxide were used at elevated temperatures to generate sulphided carbon surfaces on a variety of sp² substrates. Structural data revealed in all cases the absence of graphitisation phenomena although the reaction temperatures were up to 1173 K. XPS and IR data

allowed the conclusion that two types of species were formed. One type should be C=S bonded to aromatic rings and the other one a thiolactone.

Carbon- halogen groups are well known to exist with fluorine, chlorine and bromine. These groups can be attached by redox reactions involving the halogen elements either in aqueous solution or in the gas phase. At elevated temperatures bulk reactions occur under intercalation and eventually under formation of bulk covalent carbon-halogen materials (CF_{1.1}, solid, CCl₄, gaseous) [140]. At lower chemical potential of the halogens, substitution reactions into C-H bonds (reaction 8) or addition reactions onto in-situ formed unsaturated bonds (reaction 9) occur. These two reactions are one of the most important analytical tools in describing the chemical reactivity of carbon materials. On the basis of extensive experiments with various carbons [141] the reaction of a carbon with aqueous bromine is suggested to serve as reference experiment for the quantification of the unsaturated carbon atoms which are mostly masked by oxygen surface groups (reaction 9).

The reaction with chlorine occurs after high temperature outgassing directly as addition of halogen on the unsaturated C=C bonds. The strength of the carbon - halogen bonds is determined by using halogen saturated carbons for halogenation of nucleophiles [33]. It occurs that iodine groups are fully reversibly adsorbed whereas bromine and chlorine are partly irreversibly adsorbed and can only be removed by high temperature treatments under oxidising or reducing conditions. This result led to the conclusion that aqueous iodine solutions should be used to determine the surface area of carbon as selective adsorbent. Reaction with iodine vapour at elevated temperatures (600 K) results in the same chemistry as shown in reactions 8,9 and is not suitable for carbons selective surface area determination.

Care has to be taken when interpreting results of halogen uptake on carbon at low temperatures, in aqueous solutions or at undefined surface states of the carbon ("as received"). A large number of reactions involving halogens and oxygen surface functional groups and of course between halogen hydrogen acids and basic functional groups occur simultaneously with the reactions mentioned above. They may thus perturb the analytical data (in particular the amount of HX as measure for reaction (8)) to such an extent that no meaningful result can be obtained. The only precaution is to define the surface chemistry of the carbon by pre-annealing and treatment in the gas phase or by in-situ co-oxidation [142] forcing reaction (9) to dominate.

2.1.10.15. Surface Oxygen Groups

The abundance of oxygen atoms on carbons varies over a wide range with a maximum at about C₄O (see Table 4). The surface chemical and hence many technical properties of carbon materials (including diamond [143]) depend, however, crucially on the carbon-oxygen chemistry which

controls adsorption, adhesion and oxidation activities of the surfaces. According to the reaction with liquid water one can discriminate acidic and basic surface complexes. Under almost all catalytic conditions both types of oxygen groups are present simultaneously and the pH value of an immersion of carbons in water is the result of protolysis of solid acids and solid base groups. The pH can be as low as weak mineral acids indicating that a significant solid acidity can be present on carbon. The basic reaction is rather more limited and rarely exceeds the value of pH 8. For this reason, an overall good quantitative correlation between pH in aqueous solution and analytical oxygen content for a carbon species has been established [144]. A consequence of the Brønsted acid functionality is that many of the carbon-oxygen groups exhibit a cation exchange capacity and a simultaneous anion exchange capacity (from the basic groups). These functions are most relevant for the application of carbon as catalyst support and provide a method for anchoring metal ions by the same way as used for oxide supports also on carbons. For the special case of protons (exchange on basic groups) the graphene layer in its unperturbed “aromatic” state is sufficiently “basic” to allow direct adsorption [145]. In catalytic situations this problem is of limited relevance as for high surface area material the abundance of graphitic surface patches is low and on graphitic materials the surface area is often low so that only in graphitised carbon blacks a significant interference with the determination of basic functional groups is to be expected. When the hydrogen adsorption method is used, however, to determine the dispersion of small metal particles the sorption capacity of the support for activated hydrogen (spill over) has to be taken into account.

The dominating importance of the oxygen functional groups has led to significant efforts to devise preparation routes to obtain only part of the wide pK_a spectrum on the surface, i.e. to prepare either only acidic or only basic functional groups. This was, however, only partly successful with the result that in all circumstances a spectrum of neutralisation equilibria rather than a single pK value characterised a carbon surface. Basic functional groups can be obtained when carbons are annealed in vacuum or inert gas (Ar, not nitrogen) at 875 K for several hours, cooled down under inert conditions to 300 K and then exposed to air, water or oxygen [146]. The basic reactivity occurs only after contact with water molecules which contribute to the formation of the basic groups.

Predominantly acidic groups are obtained by heating carbon in air or oxygen to 600 K -900 K with a decrease in acidity with increasing temperature (self-gasification). Very strongly acidic groups can be obtained with low-temperature liquid phase oxidation using hydrogen peroxide, ozone, chromic acid or aqua regia.

The characterisation of the resulting surfaces has been problematic ever since the early attempts [143,147] at applying chemical means. The advent of many surface physical methods has not contributed significantly more information than obtained with chemical probe reactions

(derivatisation as in the early days of organic chemistry). The reason for this is the small abundance of a wide variety of chemically different species. Most surface spectroscopies are too insensitive for the variations in chemical environment. Others require single crystal surfaces which cannot be functionalised. Vibrational spectroscopy is hampered by the strong bulk absorption of light. Nuclear magnetic resonance has relaxation problems with non-hydrogen carrying surface groups bound to aromatic graphene structures. For these reasons the bulk of our knowledge about the structural details of carbon-oxygen functionalities stems from chemical experiments as they are collected in several reviews [33, 146,148,149,150, 32]. A special series of publications is devoted to structure and reactivity of basic oxygen groups [151,152,153,154]. The following description is a critical summary from this large body of information which contains plenty of references to the original work with ample experimental details.

The analysis of the structural chemistry of oxygen groups with chemical methods is limited to stable configurations and misses by definition all metastable configurations which may, however, be present under in-situ oxidation conditions. Chemical structures of reaction products of the reaction sequence (1-7) may be found in this description but other less stable configurations may also exist. Care should be taken to transfer the knowledge reported here directly to the actual discussion about the atomic structure of oxidation reaction intermediates [155,86,122].

The acidic functional groups can be characterised by their neutralisation reactions with a selection of bases differing in their pK values. The usual reagents are sodium hydroxide, sodium carbonate, sodium bicarbonate and for very weak acids sodium ethoxide in alcohol. An additional dimension of information can be obtained by pre-treating the carbon prior to neutralisation analysis [156].

Figure 21 shows the representations of the fundamental structures responsible for Brønsted acidity. Only the groups (1) and (4) are sternly acidic in water with the anhydride hydrolysing to two carboxylic acid functions. These two groups contribute mainly to the reaction with sodium hydroxide but react of course with all weaker and stronger bases than hydroxide. The lactone groups need to undergo ring opening in a basic medium which can be achieved by 0.05 M sodium carbonate. Phenolic groups ((2) in Figure 21) are supposed to be frequent due to their structural simplicity (reaction product of oxidation step (4) in the general scheme). Their acidity is limited in water and will depend strongly on neighbouring functional groups. Sodium ethoxide is a selective reagent for their detection.

Some oxygen functional groups do not react with water molecules and behave thus as “neutral”. Their fundamental structures are shown in Figure 22. Some carbonyl groups can still react with sodium ethoxide. The ether or xanthene structure is fully inactive in aqueous media. Both neutral structures are believed to occur frequently due to their structural simplicity and the fact that

in any oxidation reaction these structures have to occur as intermediates in ring destruction sequences. In quantitative studies where the oxygen content is compared to the sum of all neutralisation reactions a significant excess of chemically unreactive oxygen is stated [149,146] which is accounted for by these neutral functions.

Broensted- basic groups are of complicated structure as can be seen from Figure 23. They consist of two interacting oxygen centres [157]; one of which is active in proton adsorption and the other one in anion exchange. The interrelation has been shown in a series of elegant chemical reactions [151,152,153,154]. The structure shown in Figure 23 is tentative, representing the simplest configuration and may have more complicated isomer structures. It is interesting to note that during formation of the basic groups a non-stoichiometric amount of hydrogen peroxide is formed when the oxidised carbon is contacted with moisture or water. This reaction which was also discussed in conjunction with an oxidation of ether structures to chromene groups [157] is reminiscent of the anthraquinone catalysis of technical hydrogen peroxide synthesis. It should be taken into account that in all situations in which dry oxidised carbons are contacted with water a chemically detectable amount of hydrogen peroxide will be formed which may interfere with experimental observations.

Suitable reactions for the chemical identification of fundamental surface groups are collected in reactions (10) - (25) which summarise convenient reactions for chemical group identification. A large number of additional reactions with rather special applications can be found in the review literature. When these reactions are used, it is advisable to test the reaction conditions by several different reactions characteristic for the same functional group. It occurs that the neutralisation kinetics can be slow, in particular with hydrophobic and porous carbons. Reaction times should not be under 24 h at ambient conditions. On the other hand, artefacts such as glass adsorption, reaction with traces of air and the intrinsic problem of conversion of the surface functional groups during chemical reaction limit the reaction time to an optimum for complete but artefact-free determination.

Reactions (12) - (15) describe the standard neutralisation reaction for an organic carboxylic acid. The discrepancy in neutralisation capacity for the different reagents can be used to estimate the pK distribution [88]. Amounts between 50 and 500 μeq acid per g carbon are characteristic values which indicate the high degree of experimental perfection required to determine such surface acidity data. Reactions (10) and (11) form derivatives of the carboxylic acid and can be used to volumetrically detect their presence by monitoring the gaseous reaction products.

Phenol groups are determined by the difference of the neutralisation reactions between sodium hydroxide (reaction (21)) and sodium carbonate (reaction (15)) which are common for carboxylic and phenolate groups. Oxidised carbons (air, 700 K, typical data) contain equal amounts of these two functional groups. Activated carbons contain up

to 800 $\mu\text{eq/g}$ carbon of phenolate groups. The volumetric determinations are also sensitive to both carboxylic and phenolate groups (reactions (19) , (20)) so that specific derivatisation processes are needed (reactions (16) , (17)) to reliably discriminate the two types of groups.

With more complicated structures such as lactones the identification problems become more complex as the reaction of lactones in water result in the formation of a carboxylic acid group and a neighbouring phenole group. The reactions (23) - (25) are only characteristic for lactones with the assumption that under the mildest possible reaction conditions the neighbourhood effects of the ring opening reaction will favour the derivation over the same reaction occurring on additionally present non - correlated functional groups.

The complexity of the chemical situation increases further when combinations of different surface groups start to react with each other. A prominent example is the lactole group originating according to reaction (26) from combination of a carboxyl group and a carbonyl group. This is a situation which is frequent due to the high abundance of both fundamental groups. The resulting structure, representing a complicated example of a co-adsorption effect, can undergo a whole spectrum of reactions and interfere with several derivation reactions simultaneously.

Another type of complication arises from the chemical inequivalence of (110) and (1-10) terminating surfaces referred to as zigzag and arm-chair configurations of the graphene layers. In reaction (27) an arm-chair configuration exhibiting two different functional groups at one six-membered ring is shown. The resulting structure, using the same fundamental groups as for the lactol reaction which are now in 1-2 configuration with respect to each other (1-1 configuration for the lactol), allows tautomerism with the result that upon neutralisation either one or two equivalents of base will be consumed. The equilibrium between the two forms depends upon the base concentration of the base used for detection.

Reaction (27) is also a good example for the insensitivity of thermal desorption for such effects as the same molecule results after decarboxylation. Any quantitative correlation between neutralisation and thermal desorption thus leads to inconsistencies which is the historic reason for the intensive investigation into this surface chemical problem [33].

These few examples give an impression about the chemical complexity of the carbon-oxygen surface reaction. They illustrate that surface acidity as a single number of sample characterisation is a very poor representation of the spectrum of reactivity already present in aqueous media. It becomes apparent why in practical applications [130,158,150] only poor correlation are observed between such simplified surface chemical parameters and the observed reactivity.

In recent years a simplifying attempt to overcome this complexity was to analyse carbon by TPD and to integrate the total CO and CO₂ emission and to correlate

the results with sample pre-treatment and chemical reactivity [33]. The limited validity of such an approach is apparent. As is illustrated below, the chemically complex surfaces which are not described by such crude correlations are those with the highest catalytic activity. In applications of carbons as catalyst support it is immediately apparent that the details of the carbon-to-metal interaction depend crucially on such details of surface chemistry. This explains the enormous number of carbon supports commercially used (several thousands). A systematic effort to understand these relations on the basis of modern analytical capabilities is still missing.

In this situation a variety of techniques can be used to obtain complementary and if possible quantitative information on the surface chemistry of a given carbon material. High sensitivity and chemical selectivity are characteristic for titration methods of the solid-acid surfaces. The most prominent technique is a one- or two point titration with two fixed concentrations of e.g. 0.05n and 0.5 n bases. The titration is usually carried out as back-titration after an adsorption experiment. The results usually differ from each other indicating the distribution of acid sites over one order of magnitude in pK values. The reactions (21) and (12) are associated with these two values. For a variety of different carbons the characteristic concentrations for the predominant analysis of carboxylic acids and phenols may differ due to variable distributions of local adsorption geometry. This affects, via the neighbouring group effects, the dissociation constants of the surface groups and hence modifies the pK distribution. To avoid the possibly substantial errors, it is highly recommended to determine the adsorption isotherm of the neutralisation reagent on the carbon and analyse the resulting data in terms of a multiple Langmuir chemisorption model.

The Langmuir model describes for a uniform surface and a non-self-interacting adsorbate the relation between adsorbed amount and exposure concentration. The parameters of the model are the maximum amount adsorbed as a full monolayer and the equilibrium constant for the adsorption-desorption process which reflects indirectly the strength of the adsorbate-substrate interaction. For the present situation the analysis is modified in the following ways:

- it is assumed that several independent site types exists which represent acids with different pK values
- the neutralisation process is seen as an equilibrium reaction which occurs in an additive way on the different site types
- no interaction between different site types is assumed (no effects as described in (26) and (27))
- no complications with correlated equilibria for generation of the primary sites (e.g. hydrolysis of lactones or anhydrides) are taken into account.

Within these limitations the method supplies information on the absolute abundance of the fundamental solid acid sites and gives a qualitative indication about the pK average of each site. The procedure works in principle

for acid and basic sites [88]. Figure 24 illustrates an example for acid sites on a carbon black sample (FW-1 from DEGUSSA). This sample was selected as the high purity allows an unambiguous assignment of the neutralisation to carbon-bonded functional groups and the high surface area provides sufficient chemical heterogeneity for a realistic model. The top panel shows the experimental adsorption isotherms after 24 h equilibration in anaerobic conditions for the as-received sample and an extracted sample. Extraction was done with xylene and ether to remove polycyclic aromatic molecules which are chemisorbed in an abundance of less than a monolayer [39] on the carbon and passivate the genuine carbon surface. The strong effect of the extraction is clearly visible. The shape of the isotherm indicates, at least for the extracted material, some complications as a stepped curvature should not occur from a single Langmuir isotherm. As the reaction should occur in an additive way it is also not expected that the combination of several isotherms should give rise to such a feature which is absent in the as-received sample. The discontinuity is ascribed to the generation of additional functional groups by chemical reactions between the NaOH with nominally unreactive functional groups during the adsorption-equilibration process.

The lower panel of Figure 24 shows the analysis of the normalised isotherms. It occurs that two processes are superimposed in each isotherm. The break in the isotherm of the extracted carbon at around 0.1 n concentration indicates that in this regime the extra reactivity which consumes base outside an adsorption probably has occurred. The data can be quantified and provides the following information. The two adsorption sites differ in their acid strengths as can be concluded from the equilibrium constants ($K = 14$ (17) for the majority site and $K = 64$ (107) for the minority sites). The limiting values of coverage are 2.32 mmol/g (3.41 mmol/g) and 1.24 mmol/g (1.74 mmol/g) for the two species. The data in brackets give the values for the extracted surface which indicate the sensitivity of the method and the drastic effect of the surface purification process. The purification has also a detectable effect on the acid strength of the sites which may be explained by the operation of neighbour group effects (adsorbate-adsorbate interaction).

The suitability of this adsorption model to characterise quantitative aspects of surface acidic groups gives no indication, however, of the chemical structure of the reactive sites. Only in combination with the chemical probe reactions is it possible to assign the two types of acid sites to carboxylic acid and hydroxyl groups respectively. It is noted that such an approach can also be used to determine ion exchange capacities for metal ion loading required for the generation of dispersed metal-carbon catalyst systems.

For carbons with large amounts of surface groups per unit weight the method of direct titration can be used. In this method a suitable arrangement for potentiometric titration with slow neutralisation, anaerobic conditions and good temperature stability of the experiment is used to

measure directly the titration curve of the solid acid. The first derivative shows the equivalence points of all stages of dissociation. The carbon is considered in this picture as an oligo-protic acid with a series of dissociation equilibria. A full description of the theory can be found in the literature [159, 33]. Figure 25 illustrates the type of information obtained from such a direct titration experiment with a carbon black sample (FW-1) which was oxidised at low temperature in liquid phase to obtain acidic functional groups. Large differences in the abundance (proportional to the peak positions on the abscissa) and in the dissociation constant (peak profile representing the shape of the discontinuity at the equivalence point relative to the strong base 0.1 n NaOH) can be seen for the two oxidising agents applied under identical conditions to the same carbon material. It is obvious that ozone treatment resulted in the formation of a large amount of very strongly acidic surface functional groups as seen from the sharp peak in the derivative plot. Three to four other types of functional groups may be identified with widely varying abundance. Care must be taken in analysing the derivative profiles as for weaker acidic systems the effect of incomplete dissociation and the formation of a buffering system which all broaden the derivative peaks must be taken into account.

Table 5: Selected Carbon 1s Chemical Shift Data for Carbon-Oxygen Groups
Common Reference is C 1s = 284.6 eV for Graphite

Binding Energy (eV)	Assignment	Surface	Reference
285.6	C-O-C	poly-vinyl-alcohol	234
286.5	C-O-H	poly-vinyl-alcohol	234
287.8	C=O	poly-vinyl-alcohol	234
289.2	CO ₂ H	poly-vinyl-alcohol	234
286.2	C-O-R	polyethylen e oxidised	174
287.5	C=O	polyethylen e oxidised	174
289.0	CO ₂ H	polyethylen e oxidised	174
286.1	C-O-H	carbon fiber oxidised	172
287.6	C=O	carbon fiber oxidised	172
289.1	CO ₂ H	carbon fiber oxidised	172
290.6	carbonate	carbon fiber oxidised	172

The direct titration of the parent carbon black which also carries significant amounts of functional groups is not possible. From this, it can be seen that the two alternative chemisorption techniques have both their relevance in carbon chemistry.

Another physical method which became popular in functional group analysis is photoelectron spectroscopy with X-ray excitation. The XPS or ESCA method is used in this conjunction as a fingerprinting tool using empirically derived tables for the chemical shift to analyse the data. Oxygen functional groups can be analysed either by the oxygen O 1s emission or by the carbon C 1s emission. Due to the much larger shift sensitivity, the carbon 1s range is used in almost all applications. In addition, the presence of a film of molecular water which is not removed in UHV creates a large oxygen 1s signal at 533 eV which overrides many structures in the functional group oxygen spectrum.

The issue of assigning carbon 1s data to chemical structures has been developed extensively in carbon polymer science and is exhaustively reviewed there [160,161,162]. The principle of the assignment resides on the following assumptions. All sp² and sp³ C-C and C-H bonds give rise to one C 1s signal at 285 eV with a tendency towards lower binding energies for pure graphite which was located for defect-poor samples at 284.6 eV [90,163,2]. All carbon heterobonds shift the C 1s signal to higher binding energy. This shift is the larger the more electronegative the heteroelement is relative to carbon. Further increments are brought about by carbon-heteroatom double bonds and by 1,1, substitution of the C-C or C-H bonds. Table 5 reports a critical compilation of literature data on carbon-oxygen induced shifts for several carbon materials. The table confirms the general trend outlined above. Other tabulations in the literature [33] are physically inconsistent and contain erroneous data. These discrepancies arise from three different sources of inconsistencies:

- calibration of the binding energy scale for different experiments (see below).
- influence of the defect structure on the absolute position of the main line which is often used as internal standard for calibration of the binding energy scale [163].
- disregard of the asymmetric lineprofile of the graphitic carbon 1s signal. This asymmetry contradicts a physically meaningful spectral deconvolution into a set of Gaussian peaks as mostly done in the literature. The resulting inconsistencies in the positions of contributions and the variable linewidths used in these deconvolution procedures arise from the varying contribution of the line asymmetry to the total spectral weight of the carbon 1s profile. The asymmetry is mainly caused by the coupling of the core hole state created during photoemission to the semi-metallic valence band states of graphite and by the convolution of the primary photoemission with the phonon and plasmon loss spectra [164,165]
- disregard of charging effects. Highly functionalised carbons are often not sufficiently metallic

conducting to allow the photocurrent to flow through the sample without creating integral potential drops which affect the position of the binding energy scale. In difficult cases the “charging up” is locally variable (with thick uneven specimen e.g.) and prevents correction by re-calibration with an internal standard (the C-H +C-C line or the water line).

These three groups of effects shift all or part of the photoemission intensity into the range of the carbon-oxygen shifts and thus affect the interpretation in often undetected way. The same problems arise when carbon-nitrogen groups are analysed. Nitrogen-oxygen groups (nitrate, nitrite, nitrosyl) are well discernible (403 - 406 eV binding energy) from nitrogen-hydrogen bonds (around 401 - 400.5 eV for amino groups) and from carbon-nitrogen bonds (values between 400.0 and 397 eV). The individual chemical configuration within the groups is, however, difficult to resolve [135]. In a recent publication [166] on the reactivity of nitrogen species with oxidised activated carbons a consistent series of nitrogen chemical shifts falling within the ranges specified above is established. This list of compounds is chemically self-consistent as the modifications used for their generation are fully in line with conventional nitrogen organic chemistry.

The C 1s line is less affected by the less electronegative nitrogen heteroatom and exhibits a much smaller shift range than for oxygen groups. In a recent publication aiming at the XPS analysis of the novel-diamond-like C_3N_4 material [167] all these problems are well documented. The authors did not consider charging effects, nor did they account for oxidation of the sputtered surfaces during transfer. In addition, they used Gaussian lineprofiles and arrived at significantly high carbon 1s chemical shifts for two different C-N bonding geometries which they see as diamond-like (aliphatic) and polypyridine-like (heterocyclic aromatic).

In a very detailed study of the chemical shifts of carbon 1s lines on the nature of the C-C bonding interaction [168] it was found that using the well-determined value of C 1s of 284.6 ± 0.3 eV [169] hydrogenated carbons exhibiting a binding energy of 285.3 (± 0.05) eV and carbicid carbon in SiC were found to occur at 283.4 (± 0.05) eV. Diamond and graphite were found to be fully indistinguishable from their shift data which is in full agreement with a different study using compact [2] rather than film [169] samples. The significant uncertainty which is quoted in the literature for the value of graphite C 1s photoemission was clarified in a study on the dependence of the carbon 1s line position on the crystalline quality (nature and abundance of surface defects) [163]. For hydrogenated amorphous carbon films a complex influence of the substrate on the binding energy and probably also on the detailed atomic structure was detected in a study of a-C-H films on various GaAs surfaces. A carbon-rich species with a binding energy of 284.8 eV on GaAs and of 284.6 eV on Si was found in the near interface region of sputtered thin carbon overlayers [170]. These data

indicate that a clear speciation of the chemical structure of a carbon species in a catalytic system can be quite ambiguous and that- contrary to chemical intuition- the connectivity of a carbon cannot be inferred from its carbon XPS spectrum. The reason for this failure of the “ESCA” effect lies in the complex convolution of ground state electronic properties of the carbons (which are all different [2] as expected by intuition) with final state effects [164,165] (relaxation of the core hole) which produce a diffuse but intense structure in each peak accounting for their apparent similarity. This became apparent in studies aiming at a discrimination of the KVV Auger spectrum of carbon into s-derived and p-derived valence band states which should be suitable to discriminate sp^3 and sp^2 carbon connectivities by the Auger lineshape [171].

In summary, care must be taken in interpreting the main component of the carbon 1s line as fingerprint for the carbon connectivity. In the high binding energy side additional problems arise from plasmon satellites which can occur at 5.6 - 7.2 eV in sp^2 carbons and at 11.3 eV-12.5 eV in sp^3 carbon above the main line [169]. These broad and weak structures interfere with chemical shift identifications of highly oxidised C-O functional groups [163].

A practical situation is shown in Figure 26. The carbon 1s data of HOPG as reference are compared to those of a chemically etched graphitised carbon black sample. The defective graphitised carbon surface exhibits a significantly wider main line at almost the same position as the well-ordered graphite (cleaved and annealed in UHV [90]). It can be seen that the neglect of the line asymmetry invariably causes the erroneous detection of additional lines in the range 1-2 eV above the peak maximum. The difference spectrum is mainly caused by the broadened main line. Only after removing the asymmetric main contribution a small structure (top in Figure 26) can be isolated revealing peaks at 286.0, 287.3, 288.7 and 290.0 eV which can be attributed to surface oxygen functional groups. Only 4.3% of the total intensity is due to the surface groups which is in good agreement with 5.5 at% oxygen content. The comparison of these numbers allows one to conclude [172] that most functional groups can only carry one oxygen atom per carbon atom and that carboxylic groups with the largest shift must be a small minority. The data agree fairly well with those from oxidised carbon fibers [172] and are in agreement with the values from Table 5. A maximum of three different oxygen functionalities can be resolved by XPS. These are the basic chemical structures mentioned above. The more complex cases which were shown to exist with carbon-oxygen single bonds (peak at 286.0 eV in Figure 26) can also not be resolved by this method with any degree of chemical accuracy.

A significant increase in the chemical specificity of XPS can be achieved when the surface sensitivity of the surface analytical detection is combined with the chemical specificity of the probe reactions discussed above. A highly specific analysis of the chemically reactive surface

functional groups can be obtained using heteroatoms like barium from barium hydroxide and chlorine from HCl or SOCl_2 [173] or nitrogen and sulphur tags from complex functionalisation reagents [174,175]. These data reveal that a large number of oxygen functions detected by integral elemental analysis are chemically inert and exhibit no acid-base activity. Such behaviour is consistent with keto functions or with oxygen heterocyclic functions (C-O-C in Table 5). From all chemical shift data in the literature and the spectrum in Figure 26 it appears that the heterocyclic function is the dominating functional group. This accounts for much of the analytical oxygen content without contributing to the low-temperature chemistry. From the sequence of events in carbon oxidation this group is the primary reaction product and has thus also from the mechanistic point of view a high probability to survive any oxidation treatment as the most abundant reaction intermediate.

At this point a characterisation technique with a higher chemical resolution is desirable as such functionalisation plus surface analytical combination experiments are extremely difficult to perform in a clean and reproducible way. Vibrational spectroscopy such as the FT-IR technique has developed in recent times into such a tool after several methodical improvements concerning sample preparation and detector sensitivity. In-situ oxidation experiments are still very difficult as heated black carbon is a perfect IR emission source and interferes with any conventional detection in the spectral range of carbon-oxygen fingerprint vibrations.

A compilation of fingerprint vibrations for characteristic carbon-oxygen functions is found in Table 6. Data from a variety of organic molecules from spectra libraries are analysed and grouped together. Only strong vibrations are tabulated and extreme positions are removed. The compilation shows that several regions of interest exist:

- the OH- valence region which is due to combinations with molecular water often difficult to resolve
- the C=O region (1800-1650 wavenumbers)
- the region at 1650 wavenumbers, of C=C vibrations which are isolated from the graphene network (the graphene vibrations are only Raman active, see Table 2)
- the region of C-O single bond vibrations at 1300-1100 wavenumbers with a significant selectivity for different groups when combined with the simultaneously occurring C=O vibrations.

The practical observation of all these vibrations is difficult, as not all of the respective groups are present on a carbon with the same relative abundance. As the quality of the spectra is generally poor, weak characteristic peaks of a minority group may not be recognised. Strong peaks at 2355 cm^{-1} and at about 2045 cm^{-1} arise from chemisorbed CO_2 and carbon monoxide during in-situ studies [176,177,178]. The diagnostic value of the data in Table 6

is enhanced by the search for combined absorptions for the more complex functions. Such combinations allow the resolution of the crowded spectral range between 1800 and 1700 cm^{-1} . Two spectra of oxidised carbon samples are discussed as being representative for the many possible applications of Table 6.

Table 6: Characteristic group frequencies in IR absorption

functional group	absorption frequency (cm^{-1})	assignment
phenol groups		
O-H	3650 - 3590	valence
O-H	3500 b	valence polymer
C-OH	1220 - 1180	valence
C-OH	1350 - 1100	valence aliphatic
O-H	1390 - 1330	deformation
keto groups		
C=O	1745 - 1715	valence aliphatic
C=O	1700 - 1680	valence aromatic
C=O	1730 - 1705	valence alpha diketo
quinones		
C=O, para	1690 - 1655	valence, two lines
C=O, ortho	1660	valence, one line
aldehyde groups		
C-H	2920 - 2880	valence, combined
C=O	1720 - 1715	valence, combined
carboxylic acids		
C=O, aliphatic	1735 - 1700	valence
C=O, aromatic	1700 - 1680	valence
C=O, anhydride	1830, 1750	valence, two lines
O-H	3000 - 2700	valence
O-H	940 - 900	deformation
ester, lactones, ethers		
C=O	1730	valence, benzoic
C=O	1740	valence, lactones
C-O-C	1280 - 1100	valence, ester, lactones
C-O-C	1320 - 1250	valence, ethers

The discussion of characteristic IR data on fullerenes and their oxidation products can be found in the literature [108,105,106,111]. Table 7 lists the main absorption frequencies for the two samples. One is a disc of glassy carbon formed under electrochemical oxidation, the other is a powder sample of a high surface area carbon black (FW-1, 235 m^2/g). The in-situ electrochemical oxidation study [176] allows the tracing of several co-existing species by their respective fingerprints. It can be

seen that several groups which remain undetected by chemical adsorption and XPS analysis can be found with the IR technique. No carbon-oxygen single bonds were found in this study. The oxidation potential may have been too high for the accumulation of a significant abundance of these still oxidisable groups. A technical reason may well be the poor spectral quality below 1600 cm^{-1} precluding the detection of any specific absorption besides the extremely strong background. The broad water hydroxyl peak from the in-situ reaction environment also does not allow the detection of hydrogen groups. For these reasons, not all species are identified. This is required to derive a plausible oxidation mechanism suggested in this paper.

The oxidation reaction by dry ozone at 335 K leads to the formation of a large number of strongly acidic surface groups [179]. A whole spectrum of chemical changes occurs with the treatment leading finally to a break-down of the carbon into soluble graphene fragments. The ozone reaction is also used to study the oxidation mechanism and its control by micromorphological effects of "hole burning" [180]. Finally, the ozone oxidation is also of influence in atmospheric chemistry, where it modifies carbon black particles which become efficient catalysts for the oxidation of SO_2 under ambient conditions [181].

The data from Table 7 and the spectrum in Figure 27 indicate that a wide variety of functional groups with single and double oxygen-carbon bonds are formed after mild ozonisation at 335 K in aqueous medium. The agreement between the assignments of the absorptions in both samples is quite remarkable and agrees also with the reference data in Table 6. The operation of neighbourhood effects on vibrational data and the uncertainty of locating the position of absorptions in broad, overlapping and diffuse bands account for the discrepancies in the numerical values of the peak positions. The regions of characteristic absorptions mentioned above can be well recognised in the top spectrum of Figure 27. A distribution of absorption band positions for each chemical structure causes the broad envelopes and indicates the structural heterogeneity of the oxidised carbon surface. The sharp double peak of gaseous CO_2 arises from the large micropore volume of the sample which stores detectable amounts of CO_2 in relation to the natural abundance of this gas in the ambient air.

The nature of the functional groups seems not to depend on the structure of the carbon substrate, as even on oxidised fullerenes the same bands can be found by IR spectroscopy [108]. The relative abundance is, however, significantly different as can be seen from the comparison of the two carbon black samples used for the data of Figure 27. The FLA 101 is more graphitic with a significantly reduced surface area. The abundance of carbon-oxygen single bonds is greatly reduced with the predominant species being carboxylates after the same treatment which produced on FW-1 the broad variety of functional groups. This is full agreement with the mechanistic picture in the literature [180] which correlates velocity and depth of

oxidation with microstructure and porosity of the carbon substrate.

Table 7. Observed IR absorption bands for oxidised carbons

oxidised glassy carbon		oxidised carbon black	
absorption frequency (cm^{-1})	assignment	absorption frequency (cm^{-1})	assignment
2045	adsorbed CO	3425	C-OH
1780	lactones	2924	C-H aliphatic
1722	carboxylic acids	2355	CO_2 gas phase
1696	aromatic ketones	1760 sh	lactones
1678	quinones	1729	carboxylic acids
1611	isolated C=C bonds	1620	isolated C=C bonds
		1438	O-H deformation
		1399	C-O lactones
		1230 sh	C-O aromatic ether
		1210	C-O phenol

Vibrational spectroscopy is a very versatile and, chemically, well-resolved technique to characterise carbon-oxygen functional groups. The immense absorption problems of earlier experiments seems to be overcome in present times with modern FT-IR, DRIFTS or photoacoustic detection instruments. The physical technique of desorption spectroscopy of oxygen functional groups is much more frequently used. The conceptually simple experiment using a carrier gas and a non-dispersive infrared detector for CO and CO_2 respectively is not in line with theoretical complexity of the experiment. One group of complications is of technical character and refers to carrier gas purity, mass transport limitations, temperature gradients, non-linear heating ramps and temperature measurement problems. More severe is the problem that the method is destructive in two ways. First, it removes the functional groups and has to break all adsorbate-substrate bonds in a distribution of local geometries. Secondly, it is a high temperature process which activates functional groups to change their structure during the experiment and to interconvert into each other. This is particularly complicated in situations with carbon-oxygen single and double bonds located next to each other (see e.g. lactone decomposition exemplified in reaction (27)).

Despite these principal ambiguities the thermal desorption method is a standard characterisation technique in carbon surface chemistry. Various examples and data about desorption profiles for a selection of carbon treatments can be found in the literature [88,90,182,183,155].

The general features of all these data can be discussed using the experiment shown in Figure 28. A highly reactive carbon with complex amorphous structure was treated with ozone at 335 K in water and the dried product subjected to a temperature-programmed decomposition in flowing nitrogen using a special mass spectrometer (IMR-MS) as detector. This instrument [184] allows the suppression of the nitrogen signal and fully removes any fragmentation of CO₂ into CO. This is a problem which is significant in conventional mass spectrometers allowing only crude estimates of changing ratios of CO to CO₂. From Figure 21, it occurs that the acid groups (1), (3) and (4) result in CO₂ as decomposition products while all other surface groups produce mainly CO during their pyrolysis under non-oxidising conditions. The more strongly oxidised alpha-carbon atoms in acidic groups desorb from the graphene surface at lower temperatures than the CO from the basic groups. This behaviour can be recognised in the IMR-MS traces of Figure 28. The CO₂ trace shows structures in three broad features with the first peak exhibiting some internal structure which is ascribed to the decomposition of free carboxylic acid groups and structures with other functions next to the acidic group (reaction 27). The poor resolution of the main features indicates significant kinetic effects at a heating rate of 0.5 K/s which points to a distribution of binding energies rather than to one specific desorption event. The occurrence of post-desorption reactions of the CO₂ acting as oxidant for other functional groups has to be taken into account at temperatures above 650 K [112]. This finds its expression in the crossing-over of the (sensitivity-corrected) desorption traces around 650 K. The increased stability of the basic and neutral functional groups is seen in the high-temperature rise of the CO trace which peaks only above 1000 K. At these temperatures the structural rearrangement of the graphene layers in amorphous carbon becomes an important process which prevents the observation of the complete desorption of all oxygen functional groups without changing the bulk structure of the substrate. Structural changes in the substrate give rise to the “noisy” appearance of the CO trace which indicates eruptions of gas due to the beginning “hole-burning” process initiated by local concentration maxima of surface oxygen species which terminate quickly due to the lack of oxidant.

The desorption of oxygen functional groups is not correlated with the steady state burn-off of the material in molecular oxygen which begins at temperatures significantly above the desorption of predominantly highly oxidised functional groups.

The relative contributions of the different desorption processes changes with the average surface

structure. Comparison of the data in Figure 28 with those of an analogous oxidation experiment with a different carbon substrate (carbon black FW-1) shown in Figure 29 reveals that the carbon black contains significantly more basic functional groups than the amorphous fullerene black. This can be traced back to a reduced number of carbon atoms which could be highly oxidised (removed from the aromatic backbone of a graphene BSU) by ozone in the two materials. The presence of five-membered rings in the fullerene black and the organisation into stacks of planar graphene units in the carbon blacks are consistent structural explanations. In the carbon black sample, the separation into regimes of stability for acidic and basic functional groups is much less resolved. This indicates a larger structural diversity of the functional groups in the carbon black relative to the pronounced maximum of acidic groups in the fullerene black.

The lower traces in Figure 29 reveal that other desorption processes occur with the decomposition of oxygen functional groups. The polar oxygen groups bind a layer of water molecules which desorbs above 415 K, after the removal of water multilayers slightly above ambient temperature. The desorption of CO₂ from acidic groups leaves behind a C-H function. If this function is in an olefinic or aliphatic environment, i.e. in a surface without a closed carbon hexagon termination, then desorption of methane can contribute to a stabilisation of the surface by removal of the non-aromatic structures. The missing hydrogen atoms are taken from reactions of water with these defective carbon centres. The respectively small methane signal is displayed in Figure 29. No higher hydrocarbons are detectable in this experiment. A desorption of molecular hydrogen at temperatures above 900 K from the terminating hydrogen atoms with aromatic carbon structure has been observed in the literature [33].

Thermal desorption data can be integrated and may be used to quantify the total number of oxygen functional groups on a carbon surface. When these data are compared with the sum of all chemically detected functional groups a significant excess of the desorption value over the chemical value is found. This excess is confirmation for the existence of chemically neutral oxygen functions which are, in part, strongly bound to the substrate (keto functions, see Figure 22). These groups act as side blockers in surface reactions and are termed in the carbon oxidation literature [86] as “stable complexes” which inhibit the oxidation.

The data in Figures 28 and 29 reveal that it is not possible to fully detect the oxygen desorption without reaching temperatures at which structural changes occur in the substrates. This is a significant problem for hydrocarbon-rich carbons in catalytic deposits. The application of thermal characterisation methods has to be regarded with significant reservation, as severe carbonisation and dehydrogenation will go along with the “analytical” desorption events. In subsequent adsorption or reaction experiments the presence of a stable graphitic carbon as second phase is stated. The “second phase” is, in

fact, an artefact of the preceding thermal treatment. A discussion of this point which also complicates surface science experiments with oxygen on carbons can be found in the literature [88,90].

2.1.10.16 Carbon as Catalyst Support

The application of carbons in catalysis is mainly as support for active phases in various reactions. Besides a wide variety of noble-metal carbon systems for hydrogenation reactions and fuel cell applications, the large scale application in the synthesis of vinyl acetate and vinyl chloride are important technical applications [185]. An important application of carbon-supported oxides of silver and copper+chromium named “whetlerite” is as the active mass in filters for gas masks. The complex chemistry occurring upon oxidation of hazardous gases requires the presence of the carbon surface besides the oxide particles which is interpreted [186] as indication for a synergistic effect between carbon and oxides for chemisorption of the hazardous gases and simultaneous selective oxidation by activated oxygen. The special field of carbon gasification catalysis is not covered here as in this reaction the carbon is not only the support but also the substrate. The rare case of a desired consumption of the catalyst support creates a special situation [185, 187,188]. An exhaustive review about the application of carbon-supported catalysts in synthetic organic chemistry can be found in the literature [189].

In all synthetic catalytic applications, carbon is considered as a support with little reactivity towards sensitive molecules with reactive functional groups which would be activated by either Brønsted or Lewis acidity of an oxidic substrate. This so-called weak metal support interaction was questioned in a comparative study on metal support-interactions for platinum particles [190]. Unfortunately, the preparation conditions were chosen such that gasification of the support had occurred. For a detailed discussion see below. The extremely valuable advantage of an inert substrate has consequently the disadvantage that the active phase is difficult to anchor on the surface. It is hence difficult to create and maintain any useful dispersion of the active phase on carbon. An elegant way around this problem is suggested in the literature [191]. A conventional oxide-supported catalyst may be, after its synthesis, covered with a deliberate carbon contamination layer on the support oxide to shield the free support surface by a carbonaceous deposit. Chemical vapour deposition of carbon from propene on alumina carrying a technical HDS system as active phase was used as demonstrator.

Two more classical ways to anchor the active phase [36] to the substrate are the fixation on oxygen functional groups or on surface defects like steps in a basal plane of a graphitic structure. In a recent study [192] of the anchoring of the active phase on graphite, the hydrolysis of a platinum complex followed by an in-situ reduction at low temperature allowed the grafting of platelets of platinum metal with a highly preferred (111) orientation and with

high dispersion on a graphite substrate. It is not yet demonstrated that this attractive arrangement survives catalytic action under useful conditions for useful times. The system was, however, used to study the microstructure of the dispersed platinum. Figure 30 shows an STM image of a raft of platinum (area 1) on graphite (001) (area 2). It can be seen from the atomic resolution insets that both surfaces exhibit the same symmetry indicating the (111) orientation of the platinum. The distinction between carbon and platinum was made possible by the differing lattice constants. The noise in the graphite image next to the platinum raft is attributed to a contamination of the STM tip which was collected from the metal. The thickness of the platinum raft is several metal monolayers, making any accurate analysis difficult due to the imaging artefacts. The genesis of this catalytically highly desirable structure is assumed to start from a molecular anchoring of the precursor at atomic defect sites. These act as nucleation centres for the metal platelets resulting from low-temperature chemical reduction and subsequent coagulation of initially formed metal clusters with no stable anchoring at the basal plane.

The more conventional strategy is described in the literature [36,189]. It contains several steps of modification and activation:

- use of a high surface area graphite with little pore structure in which the active component can be occluded.
- creation of a maximum amount of acidic surface functional groups with cation exchange capacity.
- cation exchange of protons by metal ions or hydrolysis of metal complexes by the surface acid groups.
- chemical reduction of the metal at low temperatures.

This final activation step is often the difficult reaction step as the reduction of the active component should not reduce the anchoring sites at the carbon. This reduction can occur either chemically by hydrogen atom spill-over or thermally by decarboxylation of the anchoring group. Figure 29 reveals that this decarboxylation can occur at such low temperatures that the stability limit can easily be exceeded by a thermal reduction with e.g. hydrogen. The section on surface groups reveals that it is not possible to use stable functional surface groups for anchoring as these groups are chemically inactive and all active groups are thermally not stable.

The inherent problem of limited thermal and chemical stability of metal anchoring sites on carbon limits not only the activation temperature but also the application conditions [185]. In oxidising environments carbon supports are much less stable than the macroscopic burn-off temperature (see e.g. Figures 28, 17). In order to maintain the dispersion of the active phase, the limiting temperature should be less than the decarboxylation temperature of the anchoring groups. This temperature is equal to the beginning CO₂ evolution which sets a margin of stability of the initial dispersion to about 450K - 500 K. In hydrogenation applications the limiting temperature can be

even lower as the active catalyst can produce a stream of active hydrogen which reacts with oxidised anchoring groups under hydrogenolysis/hydrogenation even below 500 K. As, however, most hydrogenation reactions are carried out at temperatures below 373 K to maintain high selectivities, the carbon metal systems are usually not limited by thermal degradation in the case of hydrogenation reactions as these are usually carried out at temperatures below 373K to maintain high selectivities

The reactivity of carbon surfaces without functional groups is low with respect to most elements [193]. Important exceptions are molecular oxygen (see next section), dihalogens [185] and alkali metals. The redox-amphoteric behaviour of sp^2 carbon which is the basis for the intercalation chemistry [140] allows for a significant charge transfer between adsorbed alkali (or halogen) atoms and even carbon on the graphite (001) surface. Thermodynamic properties of these adsorbates [194] predict that such adlayers with sub-monolayer coverage should be stable at high temperatures against desorption and should withstand even hydrolysis in liquid water. This is of significant relevance in applications where alkali is needed as catalyst promoter and the carbon substrate serves as reservoir for its storage [195].

Recent experiments [196] with high surface area carbons and iron particles strongly reduced in flowing hydrogen at 1173 K reveal an intimate contact between iron and carbon. It is further shown that an analogous charge transfer between iron and graphite as between alkali and graphite is operative when the iron particles are flat platelets with a high interface area.

These observations mark a transition from the anchoring strategy to the geometric fixation strategy for fixation of active components on carbon. This strategy relies on the assumption that chemically stable edge sites on carbon act as geometric barriers for diffusion of catalyst particles at high temperatures where molecular anchors are already unstable. A possible additional chemical anchoring via metal carbon bonds to the dangling bonds of the terminating graphene layer reduces a possible lateral diffusion along the step edge. The best fixation is achieved when the catalyst particle digs a small hole in its fixating geometry where it uniquely fits. Such a selective etching may be achieved by the high temperature reductive treatment mentioned in literature reports about metal carbon catalyst systems [195,190, 196].

The intuitive assumption that carbon surfaces with a high surface fraction of prismatic faces (110, 100 and higher indexed orientations of graphite) would be suitable to create metal-carbon (carbide) bonds is not supported by experimental evidence. These prismatic faces are chemically too reactive and undergo facile gasification in oxygen or hydrogen leading to an geometric layer, unstable situation for metal particles, which, at reaction conditions, frequently lose their specific adsorption site and become mobile with the chance of agglomeration and deactivation. Successful high-temperature carbon catalysts are always prepared from materials with a smooth and

preferentially graphitic surface. Here, the average reactivity of the support is minimised while still providing sufficient structural defects to create mechanical anchoring sites for active metal particles. This is rationalised from experiments with platinum particles on carbon and an analysis of the dispersion versus carbon pre-treatment [197,198]. The two studies were carried out with different carbons and using different reaction conditions. Both conclude that the increase in smooth surface area (not in porosity) is an important factor stabilising small metal particles. An additional factor of increased “surface heterogeneity” is stated with different relative importance in both studies. In the present context, this influence is traced back to increasing surface defects allowing direct anchoring. For high temperature preparations (at 723 K) the strong increase in platinum stabilisation [198] is traced back to the selective etch process.

The support principle of mechanical fixation at step edges is illustrated in Figure 31 which shows Ru particles on a graphite surface. The single crystalline flake is preferentially (001) oriented but exhibits a system of step structures as revealed by the Moiré fringes (weak line contrast in the main image). The metal particles of a few nm size are platelets which are occasionally stacked above each other (top left plate in Figure 31). In the main image it can be seen how an almost regular array of particles is formed at step edges of the surface. This geometric arrangement is stable in hydrogen up to 725 K where the particles become efficient methanation catalysts for their substrate. Such geometric arrangements have led to speculations that intercalation compounds between metal and graphite may constitute an active catalyst with the particles seen in Figure 31 being mechanically bound between adjacent graphene layers. The existence of such geometries is shown by TEM [199]. The investigation of other samples discounts the existence of a fixation by intercalation. [200] The activity of the materials is traced back to particles sitting only at external step edges.

The concept of mechanical fixation of metal on carbon makes the catalytic applications at high temperatures possible. These applications require medium-sized active particles as particles in the size range below 2 nm are not stabilised enough by mechanical fixation and do not survive the high temperature treatment required for the selective etching. Typical reactions which were studied in detail are ammonia synthesis [201,195, 202,203] and CO hydrogenation [204,205,206,207]. The idea that the inert carbon support could remove all problems associated with the reactivity of products with acid sites on oxides was tested, with the hope that a thermally well-conducting catalyst lacking strong-metal support interactions as on oxide supports would result.

The picture which emerges from the studies of CO hydrogenation is that besides this “clean” case of large and active particles, a second class of small particles occurs on less graphitic surfaces. These particles exhibit different activity and more importantly a much more desirable product spectrum with a high olefin to paraffin ratio. These

iron particles are superparamagnetic and may be partially oxidised[208]. The electron deficiency which is stated in all studies for the small particles is controversially discussed as pictures of different phases or a specific charge transfer with the carbon substrate.

This raises the question about the metal support-interaction in carbons. The term “wetting” for carbon-metal interaction is used in the literature[196,206]. The usual geometry of spherical metal particles as well as chemical arguments render the formation of chemical bonds between each metal atom and the carbon substrate less likely. The case of alkali metals is an exception, but only in the limiting case of sub-monolayer coverages. The images in Figures 30 and 31 support the notion of metal rafts floating on carbon rather than resting as stable compounds. Such wetting interactions should be very stable and are in strong contradiction to the observed chemistry of metal carbon catalysts. The raft structures occur only in cases of mild preparative conditions which allow the agglomeration of primary metal clusters in a predominant two-dimensional fashion. The existence of metal particles with supposed strong interaction [190, 196] is described as always being associated with very severe chemical activation conditions. It is suggested that under these conditions a combination of selective etching with a redeposition of carbon in the interface region between support structure and metal particle occurs in the same way as described above for the carbon filament synthesis. Under these conditions a reactive non-graphitic carbon binder material cements the active particle into the substrate and thus allows for a strong metal-to carbon interaction with covalent bonds between the metal and the support mediated by the binder carbon. No microstructural data are available in the literature to support this hypothesis which would explain a large body of partly conflicting results about location and stability of metal-carbon catalysts.

The whole range of carbon interactions with active phases is summarised in Figure 32. In all cases no strong chemical interaction is assumed between the graphene (001) layers and the metal platelet. The weakest interaction with, however, the highest possible dispersion is obtained with surface anchoring via functional groups. Better stability at low loading with smaller dispersion can be obtained by mechanical fixation. This process requires a flat geometry and thus selective removal of all surface impurities which frequently cover basal planes of graphitic carbons. An example of the application of platinum particles on carbon in selective NO reduction was made. [209] It was concluded from kinetic arguments that the platinum behaves identically to model single crystals with preferred (110) orientation. This can be seen as an indication for the weak metal-support interaction and for the usefulness of non-highly dispersed metal supported systems in selective reactions.

Significantly higher stability is obtained when larger agglomerates are brought into shallow holes (monolayer etch pits) of the basal planes. The generation of such pits can be achieved by reductive gasification under

catalytic influence. An alternative to the in-situ generation is the strategy of using microporous carbons which involves depositing metal particles at the pore mouths. The usually broad distribution of pore sizes in carbons prevents, however, the complete use of all metal loaded, as some particles disappear into deeper parts of larger pores and fail to be active in catalysis due to diffusional limitations. Redeposition of carbon from hydrocarbon sources (from either catalytic reactions or the ongoing reductive etching) at the boundary between the metal particle and the carbon substrate occurs. This carbon may not be graphitic but can be of a more reactive connectivity (a-C-H for example) and thus provide chemical bonding between carbon and active particle.

The chemical fixation of metal particles onto carbon via covalent interaction is possible not only via reactive carbon molecules as in the latter case but also directly on to a sp^2 surface. This occurs, provided that the electronic structure is locally perturbed transforming the carbon from aromatic into a (poly-)olefinic structure. Such a transformation can be achieved by either introducing controlled defect sites or by synthesising carbons with structurally localised double bonds. Fullerene carbon is an example of the latter case. Oxidised nanotubes or catalytically synthesised carbon nanofibers are examples of the first case. The carbon nanofiber approach was tested in the literature in several reactions [210] and the origin of the different chemical reactivity of the same active metal on planar carbon and on nanofibers was investigated in detail. Figure 33 reveals that the bimetallic iron+copper particles exhibit similar catalytic activities in ethylene hydrogenation on alumina and activated carbon but a considerably higher activity on nanotubes. The inset in Figure 33 shows that these bimetallic particles are quite resistant against deactivation by carbon deposition when ethylene is decomposed to carbon filaments and methane + ethane. The reference catalysts are fully deactivated by the time the nanofiber catalyst has reached steady state. The most plausible explanation of a different particle size distribution of the bimetallic particles was investigated by TEM. Figure 34 shows the result. It occurs that the widest size distribution by far with a maximum for largest particles observed is found for the most active nanofiber catalyst. The narrowest size distribution with the highest dispersion is achieved on the alumina support whereas the metal-on-activated carbon catalyst still exhibits a wide distribution intermediate particles between the sizes seen on the two other catalysts. The authors claim the structure shown in Figure 30. An epitactic relationship between graphite (001) and the metal close-packed structure is anticipated. The geometric data from Figure 30 make the likelihood of a strong stabilisation of an epitactic relationship surviving the activation step in hydrogen at 673 K less likely. The bonding of a broad spectrum of particles on defects situated or created by reductive etching on the graphene terminations of the discontinuous nanofibers (made by catalytic synthesis and not via the fullerene way) shown in Figure 4 seems considerably more plausible.

This example shows that a non-oxidic support can give rise to interesting properties in active particles. The catalytic performance is not simply correlated to size distributions. The experiments presented in this section reveal how few indisputable facts are yet known concerning the metal-support interaction for carbon substrates. Interactions of the type (metal d-states) - (carbon sp^3) - (carbon sp^2) mediated via amorphous accommodation particles (Figure 32) of intermediate layers should be considered in the prevailing picture of a yet unproved epitaxy between transition metals and graphite (001) surfaces.

2.1.10.17. Carbon as Catalyst

Carbon may also be used as a catalyst without an active component supported on it. This function may overlap with the widespread application of high surface area carbons as sorbents for selective chemisorption processes which is not considered here. The application of carbon as a catalyst in its own right was reviewed several times [211,212,213]. All applications are based on the simultaneous action of two functions. The first one is the selective chemisorption of an educt at the carbon through either ion exchange via oxygen functions or directly through dispersive forces involving the graphite valence electronic system. The other function is the production of atomic oxygen (or free organic radicals in dehalogenation reactions [211]) occurring on the graphene basal faces of every sp^2 carbon material. Due to its central function in carbon chemistry this process is discussed in detail below. The conjecture that both processes play an important role in catalysis and that, in particular, surface patches with an intact graphene electronic structure act as sinks and sources of electrons in catalytic reaction steps, can be inferred from several observations discussed in the literature [211,34, 135]. The importance of the graphene layers in reactivity is still discussed rather controversially in the literature. The inertness of the basal planes in oxidation frequently dominates the chemical intuition about the stability of an "aromatic" surface.

The fact that carbon is already catalytically active at ambient conditions and in aqueous medium has led to considerable efforts in applying carbon as catalyst in the condensed phase [213]. In many of these applications the surface reactivity is given by the ion exchange capacity of the oxygen functional groups binding active ions (instead of particles) and by the simultaneous presence of delocalised electrons acting as redox equivalents. The widespread use of glassy carbon as an electrochemical surface is a special case of the use of this bi-functional property of carbon under mild chemical conditions. The irreversible oxidation under these conditions and thus the decarboxylation/desorption of surface functional groups limits drastically the application of carbon catalysts in gas phase reactions. The reactions are, in this case, kinetically very slow [214] and allow the extensive use of these

functionalities and their broad chemical variation in catalytic applications.

2.1.10.18. Case studies of catalytic applications

The catalytic oxidation of sulphurous acid in aqueous medium to sulphuric acid [138, 84] has been suggested as a probe reaction for the ability of a carbon to activate molecular oxygen at ambient conditions. Besides this remarkable property the reaction is of interest in atmospheric chemistry where it provides a sink for all non-photochemically oxidised sulphur dioxide [215]. Carbon plays a special role in this environmental application as both pure carbon and active particles (iron oxide [84] for example) anchored to carbon can act as efficient catalysts. The detailed analysis of the reactivity of various types of carbon [138] reveal that basic surface oxides (see Figure 23) are important to fix the educt HSO_3^- ion. It was found, in addition, that the activation of molecular oxygen is of kinetic relevance. A variety of surface treatments which did not modify the surface basicity have drastic effects on the reaction kinetics and affect the oxygen activation. The degree of graphitic surface area, the content of nitrogen dopants and the overall electronic structure in terms of the surface perfection are found to be influencing factors. It is suggested [138] that doping of the conduction band of the carbon with free electrons from nitrogen atoms [211] is an important factor.

The selective oxidation of hydrogen disulphide to sulphur with oxygen in the gas phase at around 400 K is an important side reaction in hydrogen disulphide absorbers used for natural gas treatments. The activated carbons tolerate a high load of elemental sulphur but are eventually deactivated by a full coverage of the activated surface with sulphur. This can be removed by high-temperature steaming. Literature reports about this reaction [216,7] are quite controversial regarding the kinetics of the reaction [216]. Different carbons with differing pretreatments and different testing conditions were applied. All papers agree on the relevance of the activation details of the carbon for the performance of the catalysts. The variation of the reaction orders between 0 and 1 for each educt makes it difficult to discuss a mode of action of the catalyst. Observations from other reactions make the model presented in a review [216] highly plausible. It is assumed that carbon produces atomic oxygen which oxidises HS^- anions present in the aqueous film residing on the polar carbon surface under reaction conditions. The promoters iodine and ferrous ions act to support the chemisorption of HS^- . A compensation effect is claimed with a perfect linear relationship between activation energy and pre-exponential factor. All these details point to a significant impact of kinetic limitations which are not given by the sequence of elementary reactions.

The reaction between phosgene and formaldehyde does not occur as a homogeneous reaction under conventional conditions. It proceeds, however, in the presence of a variety of carbons with ideal selectivity at

445 K [217]. Desorption experiments show that an intermediate adduct between the two educts is the most abundant surface intermediate. The existence of highly polar (acidic) surface groups and the absence of any d-states, which decompose both educts immediately at reaction temperature, are responsible for the success of carbon in this reaction. The reaction involves the selective breaking of a Cl-Cl bond in phosgene and is thus somewhat similar to the well-known action of charcoal in the synthesis of SOCl_2 from chlorine and SO_2 . Carbon further catalyses the synthesis of phosgene from CO and chlorine. It should be mentioned that the existence of surface oxides is not sufficient to explain the reaction as OH groups on oxides do not catalyse the reaction.

The example of selective oxidation of creatinine by activated carbon and air in physiological environments [218] shows again the relation of catalysis and chemisorption in carbon applications. The creatinine oxidation plays a role as unwanted side reaction in artificial blood regeneration during dialysis. Creatinine is the ketone to the carboxylic acid creatine which is a heterocyclic nitrogen compound. Whereas the carboxylic acid is only chemisorbed on carbons, the ketone is slowly (time constant one day) oxidised to unknown products which may be toxic. This biologically relevant process occurs only in the presence of molecular oxygen and can be poisoned by chemisorption of thiosulphate. Both indications point again to the operating property of activation of molecular oxygen under very mild conditions.

2.1.10.19. The catalytic removal of NO with carbon

One of the most interesting applications of carbon in the future may be the selective reduction of NO with a non-metallic catalyst. Several highly selective and very active metal oxide catalyst systems exist for this application. They suffer, however, from lifetime and stability problems in mobile applications such as in advanced car systems. Carbon offers several unique possibilities. First, it exhibits a self-renewing surface in oxidising and in reductive environments. This removes the problem of catalyst destruction due to sudden instabilities of the gas source. Secondly it is less sensitive to irreversible poisoning by metal adsorbates (lead, arsenic, mercury). Thirdly it may be cultivated as auto-reducing agent and may allow NO removal without a second source of reducing agent such as ammonia or propene. The technological advantage is that it is cheap and can be produced in large scale amounts. All this has been recognised in research efforts and two lines of carbon as SCR catalyst [219,220,34] and carbon as NO decomposition catalyst [221,222] have been established. The general problem is to establish sufficient activity in a carbon which is not acting as catalyst support and which is not surface-modified. Only then can the advantages of the system over oxide systems be fully exploited. Carbon as catalyst support for copper particles was also tested as a successful alternative to oxide supports [223].

In the SCR application a viable solution has been found [34] by activating the surface such that extremely temperature-resistant surface functional groups with nitrogen atoms are incorporated into the carbon. Complete conversion was achieved at 575 K in the presence of a significant excess of molecular oxygen. The successful modification is obtained from a controlled synthesis of carbons from organic precursors with glucosamine as nitrogen donor. A variety of carbon samples with other nitrogen donors and carbonisation/activation procedures also enhances the SCR activity. There is however, an unclear correlation between activity and characterisation parameters. It is interesting to note that the nitrogen modification results in a change in the interaction of oxygen with the surface: The reaction order is zero with respect to the reductant and positive with NO and oxygen. The kinetic data, expressed as a rate constant of NO conversion as function of oxygen partial pressure, reveals a higher reaction order than the square root dependence on oxygen partial pressure intuitively expected for dissociative activation. Such a square-root dependence was found in earlier experiments for unmodified carbons [138]. A second type of SCR activity is found over unmodified carbons in which the carbon acts only as adsorption platform for the reactants. This is indicated by a negative apparent activation energy [34].

The direct reaction of carbon as char, graphite or activated carbon [221,222] with NO in the presence of excess oxygen is a high-temperature process operating with full NO conversion only at about 875 K. The parallel course of the activation curve for NO removal and for oxidation is taken as indication [224] that oxygen etches active sites into the carbon which NO decomposes.

Mechanistic studies [225] lead to the conclusion that NO reacts with the carbon forming CO and surface nitrogen groups which activate the carbon to react with molecular NO under formation of molecular nitrogen and oxygen. The similarity of the relevance of nitrogen functional groups in the two reaction channels is striking as well as the importance of additional oxygen to maintain high catalytic activity. This effect is sacrificial in carbon but underlines the operation of a reaction in which defective surfaces are removed and fresh graphitic surfaces are regenerated. The relevance of the surface ordering is in line with the concept of graphene (001) surfaces acting as electron donor-acceptor sites for redox reactions. This unusual mode of operation of a catalyst in which no specific surface functional group is the key to activity but rather the availability of a defect-poor free surface has been substantiated in several studies with different kinds of carbon materials [226,227,228]. The question about the catalytic nature of this reaction, which is to a certain extent sacrificial, has been addressed in all studies and answered positively by the determination of a factor "F". This is defined as the fraction of carbon consumed in the $\text{NO} + \text{O}_2/\text{C}$ reaction. Values from about 0.25 down to 0.09 are reported in the literature for a variety of materials ranging from activated carbon to coke and coal. The reaction is thus

clearly a catalytic process. For practical considerations it should be mentioned that with this still “poor” catalysis about 11 ml of carbon are sufficient to remove 100 l of NO in a 5 vol% oxygen/inert atmosphere at ambient pressure.

2.1.10.20. The removal of carbon deposits from catalyst materials.

This subject is a special subsection of the carbon - oxygen reactivity and has been treated in some detail above. The present section summarises observations of the deactivation and possible regeneration of metal-oxide catalyst systems. It has since long been rationalised [229] that in oxidative regeneration of carbonised catalysts the transport limitations play a more important role than the chemistry of the carbon. The fact that part of the carbon is usually “non-removable” under regeneration conditions is indication of the parallel carbonisation reaction transforming disordered carbon of the CH_x stoichiometry into graphitic carbon with much higher resistance against oxidation. To control this interplay between carbonisation and oxidation a detailed analysis of the carbon deposit and a specific adjustment of the kinetic details of the regeneration are necessary for each catalytic system.

A second problem of catalyst regeneration is often the modification of the dispersion of the active component. Several studies reviewed in the literature [230,24] clarify that carbon deposition from ex hydrocarbons not only cover an active particle but may remove it from its support. This mode of carbonisation occurs effectively with metals catalysing the formation of carbon filaments (see above). Figure 35 summarises the effect. A metal particle on an oxidic support (stage 1) is removed from it by the solution-exsolution mechanism creating carbon filaments. In the initial growth stage a hollow filament results (stage 2). At later stages (3) the particle restructures under the influence of the carbon/hydrogen dissolved in it and the filament is filled by the formation of graphene layers segregating from the side facets. . This oversimplified growth history has been observed in a variety of case studies by electron microscopy [24].

In the later oxidative regeneration two cases of catalytic and stoichiometric gasification [230] have to be discriminated. In Figure 36 the respective reaction pathways are depicted in a schematic way. The catalytic way leads to a reversal of the filament generation with the effect that at comparatively moderate temperatures the initial stage of a metal particle supported on the oxide are restored. In the stoichiometric case the reaction temperature is higher leading to a preferential oxidation of the inner filler graphene layers according to the layer-by-layer sequence of events described above. During the final stage of tube-wall oxidation the relation between the metal particle and the carbon fixation is lost with the consequence that the metal particle floats on the support surface and has a chance to agglomerate and move on the support surface. Depending on the catalyst loading his loosening of

the metal particle will lead to severe structural deactivation during the first or during subsequent regeneration cycles.

This simple sequence of events can be distilled out of the reviewed observations and detailed microscopic studies performed over the years [230,24]. It is in full agreement with the fundamental aspects of the topochemistry of carbon oxidation and the apparently difficult to understand wide variation of reported sensitivities of metal-oxide catalytic systems in carbon regeneration procedures.

2.1.10.21. The activation of oxygen on carbon surfaces

The process of chemisorption and dissociation of molecular oxygen on carbon is fundamental to almost all aspects of carbon surface chemistry touched here. It is further the basis of the application of carbon as selective oxidation catalyst and is an essential part of the carbon gasification reaction (reactions 1-3). Despite this fundamental importance little reliable information on mechanism, adsorption kinetics and sticking coefficient and the orientational dependence of such data is available in the literature. This is the consequence of the fact that both reaction conditions and preparation of well-defined surfaces of carbon are incompatible with conventional UHV systems. Data on polycrystalline samples or on poorly defined surfaces are available. The following cumulative assessment is given from a selection of these data. It is pointed out that similar arguments hold for the diamond surface. Only the interaction is well studied with UHV surface science methods as this reaction controls the surface reconstruction of diamond surfaces [231,232]. Little is known about the oxidation of diamond besides the mentioned fact that oxidation and graphitisation occur hand in hand.

A set of well defined and quantitative experiments on oxygen chemisorption was carried out on a sample of preheated graphitised carbon black called “graphon”. This reference material is liberated from surface functional groups by annealing at 1000 K in UHV and subjection to oxygen exposures between 200 K and 550 K in a pressure range of 10^{-4} to 10^2 mbar [136]. These conditions are suitable for the formation of basic and neutral oxygen functional groups (see Figures 22, 23). This allows the conclusion that several chemically inequivalent species are formed. A cumulative analysis of the kinetics of adsorption reveal five inequivalent sorption processes with different time constants and activation energies between 12 kJ/mole and 50 kJ/mole. All species are atomic oxygen, as shown by isotope scrambling. Their formation creates CO and CO_2 in the gas phase. The observations can ,in agreement with the authors ,only be rationalised as an indication for the reaction of prism faces with oxygen ending in basic functional groups. The desorption of adsorbed oxygen is only possible by destructive high temperature treatment releasing at 1000 K CO and CO_2 . The adsorption and activation of molecular oxygen is

undetectable as the surface is too reactive to bind the dissociation product atomic oxygen. These findings also mean that molecular oxygen can be dissociated at 200 K on polycrystalline carbon with a small apparent activation energy of 12 kJ/mole.

According to these data no reactive atomic oxygen at low and intermediate oxygen should be present on carbon which is in clear contradiction to many chemical facts reported above. Other forms of oxygen activation must co-exist with this immediate functionalisation of prismatic faces.

A first XPS spectroscopic study was aimed at the chemisorption of oxygen at 300 K onto graphite (001) [213]. A “very small but unmistakably present” amount of oxygen was detected which we today interpret as oxygen chemisorbed at the surface defects of the sample which was not annealed prior to the experiment. A sticking coefficient for molecular oxygen at 300 K of 10^{-14} is estimated. It is found that “cleaning” the surface by Ar ion bombardment which destroys the graphite structure as we know today [163] enhances the sticking coefficient to measurable dimensions of 10^{-7} on the basal plane at 673 K. Kinetic data reveals in analogy to the “graphon” experiments a variety of “at least four different” species with binding energies between 530 eV and 533 eV. As no C 1s data were reported, it is difficult today to assign these shifts to different species.

The authors [233] later reduced the number of surface species to two and assigned carbonyl- and C-O-C species to these XPS lines. It is found that atomic oxygen, generated by a microwave discharge from NO, is effectively chemisorbed at basal planes of graphite giving rise to excessive bulk oxidation. In this study the disruption of the graphite structure upon Ar ion bombardment is demonstrated. The release of implanted Ar by subsequent oxidation is taken as an elegant measure for the oxidation kinetics. Oxidation experiments on natural diamond surfaces can be found in this paper. These surfaces behave much more inert in the as-received state and are found to become similar upon Ar etching. This is explained by ion-bombardment induced graphitisation of the diamond.

In a more recent set of experiments [90,84,163] a pre-annealed surface of pyrographite with an average (001) orientation was used to perform in-situ oxidation experiments which showed measurable conversions at 10^{-6} mbar and 900 K. The oxygen XPS data reveals at higher resolution the same two structures mentioned above. On the basis of the in-situ observation it is shown conclusively that carbon-oxygen bonds give rise to several unresolved peaks between 532 eV and 529.9 eV. The structure at 533 eV is found after low-temperature chemisorption of molecular oxygen at 78 K and during in-situ gasification at 900 K as a shoulder on the strong peak of carbon-oxygen functions. This high binding energy feature is assigned to a peroxo-like molecular adsorbate species of oxygen weakly bonded to the basal planes of graphitic carbon.

•Supporting evidence for the existence of such a weakly held precursor species to carbon-oxygen functions

comes from TDS experiments on a well-characterised graphite (001) surface [90]. The material HOPG is not of single crystalline quality and contains an uncharacterised amount of surface defects. It is, however, the best approximation to a single crystal basal surface which technically can be handled. Figure 37 shows the desorption traces for molecular oxygen and CO₂ recorded simultaneously after adsorption of molecular oxygen at 78 K. A structured desorption signal for molecular oxygen is seen at low temperatures which is associated with a chemisorbed molecular species. Variation of the heating rate does not cause a shift of the main peak indicating a low formal reaction order. The detection of a second signal around ambient temperature exhibiting considerable structure was unexpected. These structures are taken as indication for a structural heterogeneity of the adsorption sites whereas the two main peaks represent two chemically different oxygen species. The simultaneously recorded CO₂ emission indicates the following facts:

•At temperatures as low 180 K oxygen is activated dissociatively and oxidises (defect sites) the carbon (001) plane.

•This is shown by a repetition of the experiment shown in Figure 37 which is impossible on the once reacted surface. Mechanical cleavage of the sample is required to repeat the experiment.

•No unspecific adsorption of oxygen at ill-defined sites can be detected for all sites for which chemisorbed oxygen in the first experiment were blocked or removed by warming to 360 K.

•The desorptions of oxygen and CO₂ occur partly overlapping and partly alternating.

•The broad structure in CO₂ desorption indicates the existence of a variety of different reaction sites compatible with varying local geometries around the defect sites. The participation of prism faces is only possible at step edges as the large prism face area of the geometric sample block is passivated by the very first experiment with the sample. Valence band electronic spectra recorded simultaneously with the desorption experiment [90] reveal the transformation of the semi-metallic surface into a fully insulating state compatible with the creation of many surface defects on the (001) plane.

•Oxygen is activated on patches of relatively electron-rich graphitic structure and reacts at structural defects which are numerous on the mechanically cleaved surface.

The observations discussed imply that no oxygen remains unreacted with carbon above 350 K which is in line with the catalytic function of carbon exhibiting no oxidation activity at high temperatures. This precludes, on the other hand that any of the species detected so far can act as efficient precursors for carbon oxidation which begins with the emission of CO at significantly higher temperatures.

Attempts were made with powdered carbons and enlarged oxygen exposure pressures to detect further species of oxygen by thermal desorption. Results are shown

in Figure 38. The spectra were obtained from a powdered graphite with a low surface area. The arrows mark oxygen desorption peaks from a sample of high surface area carbon black (FW-1, DEGUSSA). It occurs that additional adsorbed species of oxygen exist which exhibit, during their thermal activation, a finite chance to desorb as oxygen rather than the more likely thermally activated reaction with carbon sites. A low-temperature process reacts specifically to acid sites releasing CO_2 . A broad structure and the sharp high-temperature desorption peak generate increasingly more CO than CO_2 . Only the high-temperature species has the chance to reach the prism faces and to react with freshly created defect sites. All other species react with very labile surface defects which terminate in their activity after a few reaction cycles. Considering the rough structure of carbon surfaces shown in Figure 16 this seems likely for carbons with a small degree of total burn-off as it is the case with all surface science experiments.

All experimental observations can be summarised in the following scenario of oxygen activation on carbon. Two independent pathways of activation have to be considered. Both require electron-rich adsorption sites for molecular oxygen. The electrons may be either delocalised on graphitic patches or may be localised in dangling bonds at coordinatively unsaturated defects (chemically: free radical centres). These latter sites exist only after high temperature treatment in inert conditions or as short-lived species during steady state gasification. The graphitic surface patches on carbon exist after mild burn-off (see Figure 16, after the nitrogen activation procedure discussed above and after UHV cleavage) and survive in reactive gas atmospheres like water, air, NO or halogen-containing environments as long as the rate of defect formation via “hot” oxygen is low enough not to passivate the graphitic character.

Reaction scheme (28) summarises the activation of oxygen on a radical centre. This is exemplified here as an intra-layer defect (one C-C bond missing). Two carbonyl groups are formed eliminating the radical centres. Two atomic oxygen species “O” may either subsequently oxidise the former radical centres further to a carboxylic acid site or may diffuse to other sites on the carbon. This depends upon temperature and the local structural environment of the primary radical centres.

Reaction scheme (29) illustrates the chemisorption pathway in which, after a precursor state, first a hyperoxo species and then a peroxo species is formed. The dashed bonds indicate incomplete charge transfer. Only at the final step of dissociation of the

molecular precursor states is the aromatic character of the carbon adsorption site lost. The following steps can then be the diffusion of atomic oxygen leaving behind a defective carbon site (localised double bonds) or straight reaction of the atomic oxygen with those carbons where they are chemisorbed on. In the boundary condition of high oxygen partial pressure and high temperatures or at very low temperatures the reaction schemes (28) and (29) may co-operate and thus explain the TDS observations discussed above.

Unfortunately, no quantitative data on any of these reaction steps exist which are obtained under strict control of the experimental variables as is done in surface science experiments with metallic surfaces. Any microkinetic modelling which could support in a quantitative way the picture derived so far has to await such well-defined experiments.

2.1.10.22. Conclusions

The surface chemistry of carbon is rather complex. Even on one single adsorption site several chemically inequivalent types of heteroatom bonds may form. Strong interactions between surface functional groups further complicate the list of surface chemical structures as derived for the most relevant carbon-oxygen system. An additional dimension of complexity is presented by the large variety of substrate structures of carbon which are caused by the anisotropic covalent bonding rather than by a isotropic metallic interaction.

It is not surprising that a very large body of seemingly conflicting experimental observations has been collected in the literature. A great deal of confusion can be traced back to inadequate analysis of the type of carbon under study as exemplified by the use of the term “coke” in different fields of chemistry. Another general problem is the insufficient consideration of the reactivity of many carbon species during chemical treatment or even during analytical experiments (temperature-programmed methods). The underlying problem here is the insufficient knowledge about thermodynamic phases (allotropes of carbon) and kinetically stabilised metastable structures. It is a matter of debate how many allotropes of carbon exist besides graphite and diamond. In this ill-defined situation a general description of “the chemistry” of carbon is difficult and is thus not even attempted here. The intention of the compilation of experimental data is to enable the reader to find the adequate approach to analyse the situation for a particular problem with carbon chemistry.

References

- [1] J. D. Bernal, *Proc. Roy. Soc. A*, **1924**, *106*, 749-773.
- [2] F. Atamny, J. Blöcker, B. Henschke, R. Schlögl, T. Schedel-Niedrig, M. Keil, A. M. Bradshaw, *J. Phys. Chem.*, **1992**, *96*, 4522.
- [3] T. Schedel-Niedrig, D. Herein, H. Werner, M. Wohlers, R. Schlögl, G. Francz, P. Kania, P. Oelhafen, C. Wild, *Europhys. Lett.*, **1995**, *31*, (8), 461-466.
- [4] R. Berman, in *Physical Properties of Diamond*, Academic Press, Oxford **1965**.

- [5] R. Schlögl, *Surf. Sci.*, **1987**, *189*, 861-872.
- [6] R. Schlögl, in *Graphite Intercalation Compounds II*, (H. Zabel; S. A. Solin), Springer Series in Materials Science, Springer-Verlag **1992**.
- [7] V. I. Kasatochkin, A. M. Sladkov, Y. P. Kudryavtsev, M. M. Popov, J. E. Sterenberg, *Carbon*, **1973**, *11*, 70-72.
- [8] H. Kroto, *Science*, **1988**, *242*, 1139-1145.
- [9] W. Krätschmer, L. D. Lamb, K. Fostiropoulos, D. R. Huffman, *Nature*, **1990**, *347*, 354-358.
- [10] H. Werner, D. Herein, J. Blöcker, B. Henschke, U. Tegtmeier, T. Schedel-Niedrig, M. Keil, A. M. Bradshaw, R. Schlögl, *Chem. Phys. Lett.*, **1992**, *134*, (1-2), 62-66.
- [11] C. Taliani, G. Ruani, R. Zamboni, R. Danieli, S. Rossini, V. N. Denisov, V. M. Burlakov, F. Negri, *J. Chem. Soc., Chem. Commun.*, **1993**, 220.
- [12] H. S. Chen, A. R. Kortan, R. C. Haddon, M. L. Kaplan, C. H. Chen, A. M. Muijsce, H. Chou, D. A. Fleming, *Appl. Phys. Lett.*, **1991**, *59*, (23), 2956.
- [13] I. M. K. Ismail, S. L. Rodgers, *Carbon*, **1992**, *30*, (2), 229-239.
- [14] R. A. Assink, J. E. Schirber, D. A. Loy, B. Morosin, G. A. Carlson, *J. Mater. Res.*, **1992**, *7*, (8), 2136.
- [15] H. Werner, T. Schedel-Niedrig, M. Wohlers, D. Herein, B. Herzog, R. Schlögl, M. Keil, A. M. Bradshaw, *J. Chem. Soc. Farad. Trans.*, **1994**, *90*, (3), 403-409.
- [16] H. W. Kroto, A. W. Allaf, S. P. Balm, *Chem. Rev.*, **1991**, *91*, 1213-1235.
- [17] H. Werner, D. Buback, U. Göbel, B. Henschke, W. Bensch, R. Schlögl, *Angew. Chemie*, **1992**, *104*, (7), 909-911.
- [18] J. D. Fitzgerald, G. H. Taylor, L. F. Brunckhorst, L. S. K. Pang, M. H. Terrones, A. L. Mackay, *Carbon*, **1992**, *30*, 1251-1260.
- [19] T. Belz, H. Werner, F. Zemlin, U. Klengler, M. Wesemann, B. Tesche, E. Zeitler, A. Reller, R. Schlögl, *Angew. Chem. Int. Ed. Engl.*, **1994**, *33*, (18), 1866-1869.
- [20] T. Baum, S. Löffler, P. Weilmünster, K.-H. Homann, *Ber. Bunsenges. Phys. Chem.*, **1992**, *96*, (7), 841-857.
- [21] M. Endo, H. W. Kroto, *J. Phys. Chem.*, **1992**, *96*, 6941-6944.
- [22] M. Monthieux, J. G. Lavin, *Carbon*, **1994**, *32*, 335-343.
- [23] R. Saito, M. Fujita, G. Dresselhaus, M. S. Dresselhaus, *Mater. Sci. Eng. B*, **1993**, *B19*, 185-191.
- [24] R. T. K. Baker, *Amer. Chem. Soc., Fuel Chem.*, **1996**, *41*, (2), 521-524.
- [25] M. Audier, A. Oberlin, M. Coulon, L. Bonnetain, *Carbon*, **1981**, *19*, 217-224.
- [26] S. Motojima, I. Hasegawa, S. Kagiya, K. Andoh, H. Iwanaga, *Carbon*, **1995**, *33*, 1167-1173.
- [27] W. A. de Heer, D. Ugarte, *Chem. Phys. Lett.*, **1993**, *207*, (4,5,6), 480-486.
- [28] M.S. Zwanger, F. Banhart, *Philosophical Magazine B*, **1995**, *72*, (1), 149-157.
- [29] A. W. Moore, in *Chemistry and Physics of Carbon*, (P. L. Walker Jr.; P. A. Thrower), Marcel Dekker, Inc. **1981**, p. 233.
- [30] H.-P. Boehm, *Z. Anorg. Allg. Chem.*, **1958**, *297*, 315-322.
- [31] D. L. Wertz, M. Bissell, *Fuel*, **1995**, *74*, (10), 1431-1435.
- [32] W. Ruland, *J. Appl. Phys.*, **1967**, *38*, 5585.
- [33] J.-B. Donnet; R. Ch. Bansal; M.-J. Wang, in *Carbon Black, Science and Technology*, Marcel Dekker Inc., New York-Basel-Hong Kong **1993**.
- [34] L. Singoredjo, F. Kapteijn, J. A. Moulijn, J.-M. Martin-Martinez, H.-P. Boehm, *Carbon*, **1993**, *31*, 213-222.
- [35] R. Burmeister, B. Despeyroux, K. Deller, K. Seibold, P. Albers, *Stud. Surf. Sci. Catal.*, **1993**, *78*, 361-368.
- [36] D. Richard, P. Gallezot, *Stud. Surf. Sci. Catal.*, **1987**, *31*, 71.
- [37] P. B. Weisz, R. D. Goodwin, *Carbon*, **1982**, *20*, 445-449.
- [38] P. B. Weisz, R. D. Goodwin, *Carbon*, **1983**, *21*, 517.
- [39] O. Vohler; F. von Sturm; E. Wege; H. von Kienle; M. Voll; P. Kleinschmit, *Ullmann's Encyclopedia of Industrial Chemistry*, Verlag Chemie, Weinheim **1986**, p. 95-163.
- [40] M.S. Kim, N.M. Rodriguez, R.T.K. Baker, *J. Catal.*, **1991**, *131*, 60-73.
- [41] X. X. Bi, *J. Mater. Res.*, **1995**.
- [42] H. F. Calcote, *Combustion and Flame*, **1981**, *42*, 215-242.
- [43] J. Lahaye; G. Prado, in *Chemistry and Physics of Carbon*, (P. L. Walker jr.; P. A. Thrower), Marcel Dekker, Inc. **1978**, p. 167-294.
- [44] K. H. Homann, H. G. Wagner, *Proc. Roy. Soc. A*, **1968**, *307*, 141-152.
- [45] J. H. Kent, H. G. Wagner, *Combustion Science and Technology*, **1984**, *41*, 245-269.
- [46] K. H. Homann, H. G. Wagner, *Ber. Bunsenges.*, **1965**, *69*, 20-35.
- [47] J. Lahaye, G. Prado, J. B. Donnet, *Carbon*, **1974**, *2*, 27-35.
- [48] G. P. Prado; J. B. Howard, in *Advances in Chemistry Series: Evaporation-Combustion of Fuels*, (J. T. Zung), Am. Chem. Soc., Washington **1978**, p. 153-166.
- [49] C. Bertrand, J.-L. Delfau, *Combustion Science and Technology*, **1985**, *44*, 29-45.
- [50] F. Takahashi, I. Glassman, *Combustion Science and Technology*, **1984**, *37*, 1-19.
- [51] M. Frenklach, L. B. Ebert, *J. Phys. Chem.*, **1988**, *92*, 563-564.
- [52] J. Lahaye, *Polymer Degradation and Stability*, **1990**, *30*, 111-121.
- [53] R. T. K. Baker, M. A. Barber, P. S. Harris, F. S. Feates, R. J. Waite, *J. Catal.*, **1972**, *26*, 51-62.
- [54] I. Alstrup, *J. Catal.*, **1988**, *109*, 241-251.
- [55] A. J. H. M. Kock, P. K. de Bokx, E. Boellaard, W. Klop, J. W. Geus, *J. Catal.*, **1985**, *96*, 468-480.
- [56] J. R. Rostrup-Nielsen, *J. Catal.*, **1972**, *27*, 343-356.
- [57] G. A. Somorjai, *8th International Congress on Catalysis*, Verlag Chemie, Weinheim **1984**, p. 113.
- [58] G. F. Taylor, S. J. Thomson, G. Webb, *J. Catal.*, **1968**, *12*, 191-197.
- [59] S. M. Davis, F. Zaera, B. E. Gordon, G. A. Somorjai, *J. Catal.*, **1985**, *92*, 240-246.
- [60] M. Salmeron, G. A. Somorjai, *J. Phys. Chem.*, **1982**, *86*, 341-350.

- [61] L. H. Dubois, D. G. Castner, G. A. Somorjai, *J. Chem. Phys.*, **1980**, *72*, (9), 5234-5240.
- [62] J. R. Fritch, K. P. C. Vollhardt, *Angew. Chem.*, **1980**, *92*, (7), 570-572.
- [63] B. E. Bent, C. M. Mate, J. E. Crowell, B. E. Koel, G. A. Somorjai, *J. Phys. Chem.*, **1987**, *91*, 1439-1502.
- [64] S. M. Davis, F. Zaera, G. A. Somorjai, *J. Catal.*, **1982**, *77*, 439-459.
- [65] S. J. Thomson, G. Webb, *J. Chem. Soc.; Chem. Comm.*, **1976**, 526-527.
- [66] Z. Paál, R. Schlögl, G. Ertl, *Faraday Trans.*, **1992**, *88*, (8), 1179-1189.
- [67] H. G. Karge, in *Introduction to Zeolite Science and Practice*, (H. van Bekkum; E. M. Flanigen; J. C. Jansen), Elsevier, Amsterdam **1991**, p. 531-570.
- [68] S. M. Davis, Y. Zhou, M. A. Freman, D. A. Fischer, G. M. Meitzner, J. L. Gland, *J. Catal.*, **1992**, *139*, 322-325.
- [69] G. P. Handreck, T. D. Smith, *J. Catal.*, **1990**, *123*, 513-522.
- [70] K. Moljord, P. Magnoux, M. Guisnet, *Appl. Catal. A*, **1995**, *122*, 21-32.
- [71] H. G. Karge, E. P. Boldingh, *Catal. Today*, **1988**, *3*, 53-63.
- [72] D. Eisenbach, E. Gallei, *J. Catal.*, **1979**, *56*, 377-389.
- [73] H. Marsh, in *Carbon and Coal Gasification*, (J. L. Figueiredo; J. A. Moulijn), Martinus Nijhoff Publishers, Dordrecht **1986**, p. 27.
- [74] J. Maire, J. Mering, *Chem. Phys. Carbon*, **1970**, *6*, 125-190.
- [75] R. W. Henson, W. M. Reynolds, *Carbon*, **1965**, *3*, 277.
- [76] H. Marsh; P. L. Walker Jr., in *Chemistry and Physics of Carbon*, (P. L. Walker Jr.; P. A. Thrower), Marcel Dekker, Inc. **1979**, p. 230.
- [77] T. Belz, J. Find, D. Herein, N. Pfänder, T. Rühle, H. Werner, M. Wohlers, R. Schlögl, *Ber. Bunsenges. Phys. Chem.*, **submitted 1996**.
- [78] M. Kanowski, H.-M. Vieth, K. Lüders, G. Buntkowsky, T. Belz, H. Werner, M. Wohlers, R. Schlögl, *Carbon*, **submitted 1996**.
- [79] G. Blyholder, H. Eyring, *J. Phys. Chem.*, **1959**, *63*, 1004-1008.
- [80] S. Ahmend, M. Back, J. M. Roscoe, *Combustion & Flame*, **1987**, *70*, 1-16.
- [81] Z. Du, A. F. Sarofim, J. P. Longwell, *Energy & Fuels*, **1991**, *5*, 214-221.
- [82] F. S. Feates, *Trans. Faraday Soc.*, **1968**, *64*, 3093-3099.
- [83] H. Marsh, T. E. O'Hair, R. Reed, *Trans. Faraday Soc.*, **1965**, *61*, 285-293.
- [84] F. Atamny, J. Blöcker, A. Dübotzky, H. Kurt, G. Loose, W. Mahdi, O. Timpe, R. Schlögl, *J. Mol. Phys.*, **1992**, *76*, (4), 851-886.
- [85] F. J. Vastola, P. J. Hart, P. L. Walker, *Carbon*, **1964**, *2*, 65-71.
- [86] L. R. Radovic, H. Jiang, A. A. Lizzio, *Energy & Fuels*, **1991**, *5*, 68-74.
- [87] A. A. Lizzio, H. Jiang, L. R. Radovic, *Carbon*, **1990**, *28*, 7-19.
- [88] B. Henschke, H. Schubert, J. Blöcker, F. Atamny, R. Schlögl, *Thermochimica Acta*, **1994**, *234*, 53-83.
- [89] D. Herein; J. Find; B. Herzog; H. Kollmann; R. Schmidt; R. Schlögl, *Surface Chemistry and Structure of Carbons*, ACS Symposium Series, Philadelphia **1996**, p. 148-154.
- [90] R. Schlögl, G. Loose, M. Wesemann, *Solid State Ionics*, **1990**, *43*, 183-192.
- [91] J. M. Ranish, P. L. Walker jr., *Carbon*, **1993**, *31*, 135-141.
- [92] L. E. C. de Torre, J. L. Llanos, E. J. Bottani, *Carbon*, **1991**, *29*, (7), 1051-1061.
- [93] H. Marsh, T. E. O'Hair, W. F. K. Wynne-Jones, *Trans. Faraday Soc.*, **1965**, *61*, 274-283.
- [94] J. M. Thomas, *Chem. Phys. Carbon*, **1965**, *1*, 121.
- [95] C. Wong, R. T. Yang, B. L. Halpern, *J. Chem. Phys.*, **1983**, *78*, (6), 3325-3328.
- [96] A. Cuesta, A. Martínez-Alonso, J. M. D. Tascón, *Energy & Fuels*, **1993**, *7*, 1141-1145.
- [97] B. Herzog, D. Bokern, T. Braun, R. Schlögl, *Materials Sci. Forum*, **1994**, *166-169*, 517-522.
- [98] A. Kavanagh, R. Schlögl, *Carbon*, **1988**, *26*, (1), 23-32.
- [99] R. Schlögl, F. Atamny, W. J. Wirth, J. Stephan, *Ultramicroscopy*, **1992**, *42-44*, 660-667.
- [100] D. W. McKee, in *Fundamental Issues in Control of Carbon Gasification*, (J. Lahaye; P. Ehrburger), Kluwer, Dordrecht **1991**, p. 484-514.
- [101] K. J. Hüttinger; J. Adler; G. Hermann, Nijhoff, Dordrecht **1986**, p. 213.
- [102] S. Amelinckx, P. Delavignette, M. Heerschap, *Chem. Phys. Carbon*, **1965**, *1*, 2.
- [103] H. Marsh, N. Murdie, I. A. S. Edwards, H. P. Boehm, *Chem. Phys. Carbon*, **1987**, *20*, 213.
- [104] F. M. Lang, P. Magnier, *Chem. Phys. Carbon*, **1968**, *3*, 121.
- [105] H. Werner, M. Wohlers, D. Bublak, J. Blöcker, R. Schlögl, *J. Fullerene Sci. Technol.*, **1993**, *1*, (4), 457-474.
- [106] M. Wohlers, A. Bauer, T. Rühle, F. Neitzel, H. Werner, R. Schlögl, *J. Fullerene Sci. Technol.*, **accepted 1995**.
- [107] H. Werner; M. Wohlers; D. Bublak; T. Belz; W. Bensch; R. Schlögl, in *Electronic Properties of Fullerenes*, (H. Kuzmany; J. Fink; M. Mehring), Springer Series in Solid State Sciences Vol. 117. Springer, Berlin **1993**, p. 16-38.
- [108] M. Wohlers, H. Werner, D. Herein, T. Schedel-Niedrig, A. Bauer, R. Schlögl, *Synth. Met.*, **1996**, *77*, 299-302.
- [110] K. L. Yeung, E. E. Wolf, *J. Catal.*, **1993**, *143*, (2), 409-429.
- [111] M. Wohlers; A. Bauer; Th. Belz; Th. Rühle; Th. Schedel-Niedrig; R. Schlögl, in *Surface Chemistry and Structure of Carbons*, (L. J. Radovic), ACS Symposium Series, Philadelphia **1996**, p. 108-112.
- [112] I. M. K. Ismail, P. L. Walker jr., *Carbon*, **1989**, *27*, (4), 549-559.
- [113] R. L. Radovic, P. L. Walker, R. G. Jenkins, *Fuel*, **1983**, *62*, 849-856.
- [114] N. R. Laine, F. J. Vastola, P. L. Walker jr., *J. Phys. Chem.*, **1963**, *67*, 2030-2034.
- [115] H. Freund, *Fuel*, **1986**, *65*, 63-66.
- [116] P. Biloen, *J. Mol. Catal.*, **1983**, *21*, 17-24.
- [117] R. T. Yang, C. Wong, *J. Catal.*, **1984**, *85*, 154-168.
- [118] B. Pennemann, R. Anton, *J. Catal.*, **1989**, *118*, 417-423.
- [119] F. Kapteijn, O. Peer, J. A. Moulijn, *Fuel*, **1986**, *65*, 1371.
- [120] S. R. Kelemen, H. Freund, *J. Catal.*, **1986**, *102*, 80-91.
- [121] M. B. Cerfontain, R. Meijer, F. Kapteijn, J. A. Moulijn, *J. Catal.*, **1987**, *107*, 173-180.
- [122] J.A. Moulijn, F. Kapteijn, *Carbon*, **1995**, *33*, (8), 1155-1165.

- [123] R. Schlögl, in *Physics and Chemistry of Alkali Metal Adsorption*, (H. P. Bonzel; A. M. Bradshaw; G. Ertl), Elsevier Science Publishers B. V. / Amsterdam 1989, p. 347-377.
- [124] L. Bonnetain; X. Duval; M. Letort, *Proc. 4th Carbon Conf.*, Buffalo, Pergamon Press 1960, p. 107-112.
- [125] F. Kapteijn; R. Meier; S. C. van Eyck; J. A. Moulijn, (J. Lahaye; P. Ehrburger), Kluwer, Dordrecht 1991, p. 221.
- [126] A. J. Groszek, S. Partyka, D. Cot, *Carbon*, 1991, 29, 821-829.
- [127] A. J. Groszek, *Carbon*, 1987, 25, 712-722.
- [128] F. Atamny, A. Reller, R. Schlögl, *Carbon*, 1992, 1123-1126.
- [129] F. Atamny, H. Kollmann, H. Bartl, R. Schlögl, *Ultramicroscopy*, 1993, 48, 281-289.
- [130] E. Koberstein, E. Lakatos, M. Voll, *Ber. Bunsenges.*, 1971, 75, (10), 1104-1114.
- [131] J. A. Franz, R. Garcia, J. C. Lineman, G. D. Love, C. E. Snape, *Energy & Fuel*, 1992, 6, 598-602.
- [132] M. Spiro, *Catal. Today*, 1990, 7, 167-178.
- [133] R. C. Bansal, N. Bhatia, T. L. Dhami, *Carbon*, 1978, 16, 65-68.
- [134] B. R. Puri, R. C. Bansal, *Carbon*, 1964, 1, 451-455.
- [135] B. Stöhr, H. P. Boehm, R. Schlögl, *Carbon*, 1991, 29, (6), 707-720.
- [136] R. C. Bansal, F. J. Vastola, P. L. Walker jr., *J. Colloid Interface Sci.*, 1970, 32, (2), 187-194.
- [137] R. C. Bansal, F. J. Vastola, P. L. Walker, *Carbon*, 1971, 9, 185-192.
- [138] M. Zuckmantel, R. Kurth, H. P. Boehm, *Z. Naturforsch.*, 1979, 34b, 188-196.
- [139] C. H. Chang, *Carbon*, 1981, 19, 175-186.
- [140] R. Schlögl, in *Progress in Intercalation Research, Physics and Chemistry of Materials with Low-Dimensionals Structures*, (Müller-Warmuth), Kluwer Academic Publishers Netherlands, Dordrecht 1994, p. 83-176.
- [141] B. R. Puri, R. C. Bansal, *Carbon*, 1966, 3, 533-539.
- [142] W. O. Stacy, W. R. Imperial, P. L. Walker, *Carbon*, 1966, 4, 343-352.
- [143] H.-P. Boehm, *Angew. Chem.*, 1966, 78, (12), 617-628.
- [144] M. L. Studebaker, *Rubber Chem. Technol.*, 1957, 30, 1400-1483.
- [145] C. A. L. y Leon, J. M. Solary, V. Calemme, L. R. Radovic, *Carbon*, 1992, 30, 797.
- [146] H.-P. Boehm, E. Diehl, *Z. Electrochem.*, 1962, 66, (8/9), 642-647.
- [147] U. Hofmann, G. Ohlerich, *Angew. Chem.*, 1950, 62, (1), 16-21.
- [148] H.-P. Boehm, E. Diehl, W. Heck, R. Sappok, *Angew. Chem.*, 1964, 76, (17), 742-751.
- [149] H. P. Boehm; H. Knözinger, in *Catalysis, Science and Technology*, (J. R. Anderson; M. Boudart), Springer Verlag, Berlin 1983, Chapter 2.
- [150] H. P. Boehm, *Adv. Catal.*, 1966, 16, 179-274.
- [151] H.-P. Boehm, M. Voll, *Carbon*, 1970, 8, 227-240.
- [152] M. Voll, H.-P. Boehm, *Carbon*, 1970, 8, 741-752.
- [153] M. Voll, H.-P. Boehm, *Carbon*, 1971, 9, 473-480.
- [154] M. Voll, H.-P. Boehm, *Carbon*, 1971, 9, 481-488.
- [155] H. Marsh, a. D. Foord, J. S. Mattson, J. M. Thomas, E. L. Evans, *J. Colloid Interface Sci.*, 1974, 49, (3), 368-382.
- [156] G. M. Badger, J. E. Campbell, J. W. Cook, R. P. Ruffael, A. I. Scott, *J. Chem. Soc.*, 1950, 2526.
- [157] V. A. Garten, D. E. Weiss, *Aust. J. Chem.*, 1957, 10, 309-328.
- [158] H. P. Boehm; U. Hofmann; A. Clauss, *Third Bienn. Carbon Conf.*, Buffalo, New York, Pergamon Press, Oxford 1957, p. 241-247.
- [159] A. S. Arico, V. Antonucci, M. Minutoli, N. Giordano, *Carbon*, 1989, 27, (3), 337-347.
- [160] D. T. Clark, A. Harrison, *J. Polymer Sci., Polym. Chem. Ed.*, 1981, 19, 1945-1955.
- [161] D. T. Clark, A. Harrison, *J. Polymer Sci., Polymer Chem. Ed.*, 1976, 14, 533-542.
- [162] A. Diks in *Electron Spectroscopy, Theory Techniques and Application* (C. R. Brundle; A. D. Baker) 1981.
- [163] R. Schlögl, H. P. Boehm, *Carbon*, 1983, 21, (4), 345-358.
- [164] Y. Baer, *J. Electr. Spectrosc. Rel. Phen.*, 1981, 24, 95-100.
- [165] P. M. T. M. van Attekum, G. K. Wertheim, *Phys. Rev. Lett.*, 1979, 43, 1896-1898.
- [166] R. J. J. Jansen, H. v. Bekkum, *Carbon*, 1995, 33, 1021-1027.
- [167] D. Marton, K. J. Boyd, A. H. Al-Bayati, S. S. Todorov, J. W. Rabalais, *Phys. Rev. Lett.*, 1994, 73, (1), 118-121.
- [168] D. N. Belton, S. J. Schmieg, *J. Vac. Sci. Technol.*, 1990, A8, (3), 2353-2362.
- [169] F. R. McFeely, S. P. Kowalczyk, L. Ley, R. G. Cavell, R. A. Pollak, D. A. Shirley, *Phy. Rev. B*, 1974, 9, (12), 5268-5278.
- [170] D. Ugolini, J. Eitle, P. Oelhafen, M. Wittmer, *Appl. Phys.*, 1989, A48, 549-558.
- [171] M. A. Smith, L. L. Levenson, *Phy. Rev. B*, 1977, 16, (6), 2973-2977.
- [172] E. Desimoni, G. I. Casellas, A. M. Salvi, T. R. I. Cataldi, A. Morone, *Carbon*, 1992, 30, 527.
- [173] P. Denison, F. R. Jones, J. F. Watts, *J. Mater. Sci.*, 1985, 20, 4647-4656.
- [174] L. J. Gerenser, J. F. Elman, M. G. Mason, J. M. Pochan, *Polymer*, 1985, 2026, 1162-1166.
- [175] R. H. Bradley, E. Sheng, I. S. P. K. Freakley, *Carbon*, 1995, 33, (2), 233-241.
- [176] Y. Yang, Z. G. Lin, *J. Appl. Electrochem.*, 1995, 25, 259-266.
- [177] A. M. Vassallo, L. S. K. Pang, P. A. Cole-Clarke, M. A. Wilson, *J. Am. Chem. Soc.*, 1991, 113, (7820-7821).
- [178] M. Starsinic, Y. Otake, P. L. Walker jr., P. C. Painter, *Fuel*, 1984, 63, 1002-1007.
- [179] J. B. Donnet, P. Ehrburger, A. Voet, *Carbon*, 1072, 10, 757.
- [180] V. R. Deiz, J. L. Bitner, *Carbon*, 1972, 10, 145.
- [181] W. R. Cofer, D. R. Schryer, R. S. Rogowski, *Atmosph. Environ.*, 1984, 18, 243.
- [182] L. Bonnetain, *J. Chem. Phys.*, 1961, 58, 34.
- [183] S. Matsumoto, H. Kanda, Y. Sato, M. Setaka, *Carbon*, 1977, 15, 299-302.
- [184] U. Tegtmeier, H. P. Weiss, R. Schlögl, *Fresenius J. Anal. Chem.*, 1993, 347, 263-268.

- [185] H. Jüntgen, *Fuel*, **1986**, *65*, 1436-1446.
- [186] M. S. McIntyre, G. R. Mount, T. C. Lipson, B. Harrison, S. Liang, *Carbon*, **1991**, *29*, 1071.
- [187] A. Linares-Solano, M. Almela-Alarcón, C. S.-M. de Lecea, *J. Catal.*, **1990**, *125*, 401-410.
- [188] D. Cazorla-Amoros, A. Linares-Solano, C. S.-M. de Lecea, J. P. Joly, *Carbon*, **1991**, *29*, 361.
- [189] R. L. Augustine in *Heterogeneous Catalysis for the Synthetic Chemist*, Marcel Dekker, New York **1996**.
- [190] R. T. K. Baker, E. B. Prestridge, R. L. Garten, *J. Catal.*, **1979**, *56*, 390.
- [191] S. L. Butterworth, A. W. Scaroni, *Appl. Catal.*, **1985**, *16*, 375-388.
- [192] F. Atamny, D. Duff, A. Baiker, *Catal. Lett.*, **1995**, *34*, 305-311.
- [193] R. W. Joyner, J. B. Pendry, K. Saldin, S. R. Tennison, *Surf. Sci.*, **1984**, *138*, 84-94.
- [194] C. E. Milstead, A. B. Riedinger, L. R. Zumwalt, *Carbon*, **1966**, *4*, 99-106.
- [195] S. R. Tennison, in *Catalytic Ammonia Synthesis: Fundamentals and Practice*, *Fundamental and Applied Catalysis*, (J. R. Jennings), Plenum Press, New York **1991**.
- [196] E. Hegenberger, N. L. Wu, J. Phillips, *J. Phys. Chem.*, **1987**, *91*, 5067-5071.
- [197] A. Linares-Solano, F. Rodríguez Reinoso, C.S.-M. de Lecea, O. P. Mahajan, P. L. Walker jr., *Carbon*, **1982**, *20*, (3), 177-184.
- [198] P. Ehrburger, O. P. Mahajan, P. L. Walker jr., *J. Catal.*, **1976**, *43*, 61-67.
- [199] R. Schlögl, P. Bowen, G. R. Millward, W. Jones, H. P. Boehm, *J. Chem. Soc. Faraday Trans.*, **1983**, *1*, (79), 1793-1818.
- [200] S. Parkash, S. K. Chakrabartup, J. G. Hooley, *Carbon*, **1978**, *16*, 231.
- [201] K. Aika, H. Hori, A. Ozaki, *J. Catal.*, **1972**, *27*, 424-431.
- [202] M. E. Vol'pin, Y. N. Novikov, V. A. Postnikov, V. B. Shur, B. Bayerl, L. Kaden, M. Wahren, L. M. Dmitrienko, R. A. Stukan, A. V. Nefed'ev, *Z. Anorg. Allg. Chem.*, **1977**, *428*, 231-236.
- [203] K. Kalueki, P. W. Morawski, *J. Chem. Tech., Biotechnol.*, **1990**, *47*, 357.
- [204] S. Parkash, J. G. Hooley, *J. Catal.*, **1980**, *62*, 187-188.
- [205] A. Sepúlveda-Escribano, F. Rodríguez-Reinoso, *J. Mol. Catal.*, **1994**, *90*, 291-301.
- [206] A. A. Chen, M. A. Vannice, J. Phillips, *J. Phys. Chem.*, **1987**, *91*, 6257-6269.
- [207] V. K. Jones, L. R. Neubauer, C. H. Bartholomew, *J. Phys. Chem.*, **1986**, *90*, 4832-4839.
- [208] H.-J. Jung, M. A. Vannice, L. N. Mulay, R. M. Stanfield, W. N. Delgass, *J. Catal.*, **1982**, *76*, 208-224.
- [209] K. J. Lim, M. Boudart, *J. Catal.*, **1987**, *105*, 263-265.
- [210] N. M. Rodríguez, M.-S. Kim, R. T. K. Baker, *J. Phys. Chem.*, **1994**, *98*, 13108-13111.
- [211] H. P. Boehm, G. Mair, T. Stoehr, A. R. de Rincón, B. Tereczki, *Fuel*, **1984**, *63*, (August), 1061-1063.
- [212] H. Jüntgen, H. Köhl, *Chem. Phys. Carbon*, **1990**, *22*, 145.
- [213] M. Barber, E. L. Evans, J. M. Thomas, *Chem. Phys. Lett.*, **1973**, *18*, (3), 423-425.
- [214] M. Paourbaix, *Atlas of Electrochemical Equilibria in Aqueous Solution*, Pergamon Press, Oxford **1966**, p. 450-457.
- [215] O. Timpe, R. Schlögl, *Ber. Bunsenges. Phys. Chem.*, **1993**, *97*, (9), 1076-1085.
- [216] J. Klein, K.-D. Henning, *Fuel*, **1984**, *63*, 1064-1067.
- [217] T. A. Ryan, M. H. Stacey, *Fuel*, **1984**, *63*, 1101-1106.
- [218] E. M. Smith, S. Affrossman, J. M. Courtney, *Carbon*, **1979**, 149-152.
- [219] T. Okuhara, K. Tanaka, *J. Chem. Soc. Faraday Trans. I*, **1986**, *82*, 3657-3666.
- [220] H. Yamashita, H. Yamada, A. Tomita, *Appl. Catal.*, **1991**, *78*, L1-L6.
- [221] H. Teng, E. M. Sunberg, J. M. Carlo, *Energy & Fuel*, **1992**, *6*, 398.
- [222] H. Yamashita, A. Tomita, H. Yamada, T. Kyotani, L. R. Radovic, *Energy & Fuel*, **1993**, *7*, 85-89.
- [223] L. Singoredio, M. Slagt, J. van Wees, E. Kapteijn, J. A. Moulijn, *Catal. Today*, **1990**, *7*, 157.
- [226] M. J. Illan-Gomez, A. Linares-Solano, L. R. Radovic, C. S.-M. de Lecea, *Energy & Fuels*, **1995**, *9*, 97.
- [227] M. J. Illan-Gomez, A. Linares-Solano, L. R. Radovic, C. S.-M. de Lecea, *Energy & Fuels*, **1995**, *9*, 104.
- [228] J. Mochida, S. Kisamori, M. Hironaka, S. Kawano, Y. Matsumura, M. Yoshikawa, *Energy & Fuels*, **1994**, *8*, 1341.
- [229] P. B. Weisz, R. D. Goodwin, *J. Catal.*, **1963**, *2*, 397-404.
- [230] J. van Doorn, J. A. Moulijn, *Catal. Today*, **1990**, *7*, 257-266.
- [231] A. V. Hamza, G. D. Kubiak, R. H. Stulen, *Surf. Sci.*, **1990**, *237*, 35-52.
- [232] T. Frauenheim, U. Stephan, P. Blaudeck, D. Porezag, H.-G. Busman, W. Zimmermann-Edling, S. Lauer, *Phys. Rev. B*, **1993**, *48*, (24), 18189-18202.
- [233] S. Evans, J. M. Thomas, *Proc. R. Soc. Lond. A*, **1977**, *353*, 103-120.
- [234] S. Akhter, K. Allan, D. Buchanan, J. A. Cook, A. Champion, J. M. White, *Appl. Surf. Sci.*, **1988**, *35*, 241-258.